Supporting Information

Fluorescent sulphur and nitrogen containing porous polymers with tuneable donor-acceptor domains for light-driven hydrogen evolution

Dana Schwarz, Amitava Acharja, Arun Ichangi, Pengbo Lyu, Maksym V. Opanasenko, Fabian R. Goßler, Tobias A. F. König, Jiří Čejka, Petr Nachtigall, Arne Thomas, Michael J. Bojdys*

Table of Contents

Experimental Procedures

Materials

All reactions were carried out under an argon atmosphere using a standard Schlenk techniqueCompletion of reactions was determined by TLC using silica gel (Merck 60, F-254) covered aluminium plates and visualized by UV detection. Purification by column chromatography was performed using silica gel (0.063–0.2 mm, 100 mesh ASTM) from Penta s.r.o. 4-bromobenzonitrile, trifluoromethanesulfonic acid (TFMSA) were purchased from Acros Organics. $Pd(PPh_3)_4$ and 1.6 M n-buthyllithium in hexane, and CuI were purchased from Sigma Aldrich. Ethenyltrimethylsilane was purchased from ABCR. Anhydrous $ZnCl_2$ was purchased from Alfa-Aesar. Diisopropylamine (DIA) was purchased from Sigma Aldrich and Acros Organics, and triethylamine (TEA) was purchased from Acros Organics. N,N-Dimethylformamide (DMF) was purchased as an anhydrous solvent from VWR and used without further purification.

Methods

^1H and ^{13}C **NMR** spectra of the monomers in $CDCl_3$ as well as solid state (cross-polymerization magnetic-angle spinning (CP-MAS)) spectra were recorded on a Bruker Advance 400 instrument. Chemical shifts (δ) were reported in ppm (internal standard $CHCl_3$ for liquid measurements was set at δ_H = 7.26 ppm). ^{13}C cross polarization magic angle spinning (CP/MAS) NMR experiment was carried out at a MAS rate of 12.0 kHz using zirconia rotors 4 mm in diameter. The spectrum was measured using a contact time of 10 ms and a relaxation delay of 10.0 s.
IR spectra were recorded as a KBr disk on an AVATAR 370 FT-IR spectrometer from Thermo Nicolet.
Powder X-ray (**XRD**) measurements were undertaken with Bruker D8 Advance.
Scanning electron microscope (**SEM**) images were achieved with a Nova NanoSEM 450 from FEI. EDX was measured at a voltage of 20.00 kV and a spot size of 5.0.
EDX was measured with an EDAX Metek Octane Pro Detector on a FEI Nano SEM 450.
Solid state UV/Vis measurements were undertaken with a Specord 50 plus from Analytik Jena.
TGA measurements were carried out under air and nitrogen on a Mettler Toledo TGA 1 Stare thermal instrument with a heating rate of 10 K min^{-1} and a gas flow of 20 mL min^{-1} in a 70 µL aluminiumoxid crucible.
N_2 sorption measurements were performed using a Micromeritics ASAP 2020 and Quadrasorb SI from Quantachrome Instruments. Samples for nitrogen sorption at 77 K were activated by degassing in vacuum (2 × 10−5 mbar) at 150 °C. The surface area was calculated in the relative pressure (p/p_0) range from 0.05 to 0.35. Pore size distributions were calculated for the adsorption as well as for the desorption branch using the Barrett-Joyner-Halenda (BJH) pore model. The samples were degassed at 90 °C before analysis.
CO_2 sorption measurements were performed using a Autosorb-iQ2 from Quantachrome equipped with a Quantachrome CryoCooler for temperature regulation. Carbon dioxide sorption analyses were conducted at 273 K.
Transmission electron microscopy (TEM) and selected area electron diffraction (SAED) were carried out using a JEM-1011 instrument (JEOL), operating at an accelerating voltage of 80 kV with a spherical aberration coefficient value of 5.6 mm. Images were recorded on a side-mounted CCD (charge-coupled device) camera with a resolution of 2K x 2K and with an exposure time of one second per frame and an interval of two seconds between the frames. TEM specimens were prepared by dispersing the powder samples in acetone; the suspension was then drop-coated onto a copper gird with carbon support film and later allowed to dry.
Elemental analysis (EA) (C, N and H) were performed using a PE 2400 Series II CHN Analyzer.
The **ICP-OES** measurements were performed using the SPECTRO ARCOS optical emission spectrometer (SPECTRO Analytical Instruments, Kleve, Germany) with radial plasma observation. The SPECTRO ARCOS features a Paschen-Runge spectrometer mount; the wavelength range between 130 and 770 nm can be simultaneously analyzed. An air-cooled ICP-generator, based on a free-running 27.12 MHz system, is installed. For sample introduction Cyclonic spray chamber and a Modified Lichte nebulizer was used. The following ICP operating parameters were applied: generator power 1 450 W, coolant flow 13 L/min, auxiliary flow 0.8 L/min, nebulizer flow 0.75 L/min, sample aspiration rate 2 mL/min. For calibration, commercially available multielement standard solutions (Analytika, Czech republic) were used. The concentrations of calibrated elements were 0; 0,2; 1,0; 5,0; 10,0 and 20.0 mg/L, respectively. 2 mg/L Y was used as an internal standard. All measurements were performed in 4% HNO_3 as a matrix. Sample Preparation: To prepare liquid samples for ICP-OES analysis, the solid samples were weighted (approx. 5 mg) on microanalytical balance and combusted by Schöniger method. After combustion the closed Erlenmeyer flask was treated in ultrasonic bath for several minutes. After absorption of combustion products (at least 2 h) 50 µl of 1000 mg/L Y standard solution were added (final concentration 2 mg/L/). Afterwards the liquid mixture was transferred from the glass flask in a plastic bottle. The flask was rinsed carefully with demineralized water which was added to the plastic bottle. The concentration of HNO_3 were adjusted to 4% (w/w in final volume). Then the demineralized water was added to plastic bottle to achieve the final volume of 25 mL (weighed). After mixing the solution was filtered and introduced to the spectrometer system.

Synthesis

All reactions were carried out under argon atmosphere on a Schlenkline.

Synthesis of 2,4,6-tris[4-(ethynyl)phenyl]-1,3,5-triazine – EPT

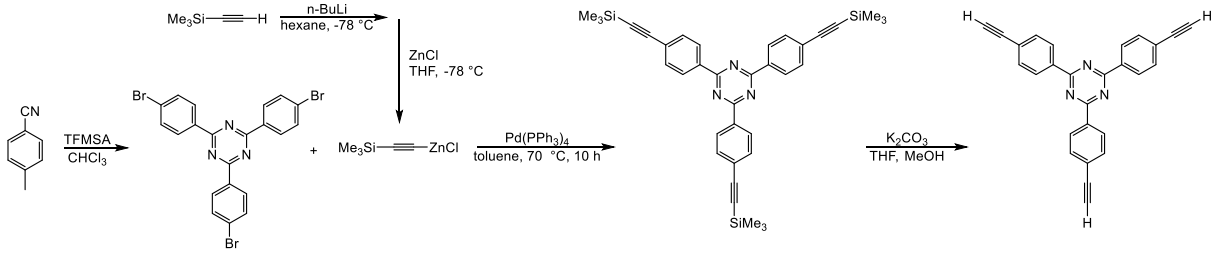

Scheme S1. Complete synthetic route of triazine-based TTF networks (CTF-TTF).

The synthesis of 2,4,6-tris[4-(ethynyl)phenyl]-1,3,5-triazine was previously reported.[1]

Synthesis of 2,2'-Bithiazole

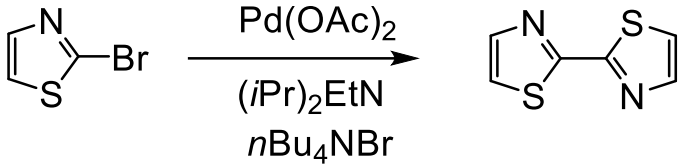

Scheme S2. Reaction scheme of 2,2'-bithiazole from 2-bromothiazole.

The synthesis 2,2'-bithiazole was carried out according to literature.[2, 3]
2-bromothiazole (0.72 mL, 1.31 g, 8 mmol, 1 eq.), diisopropylethylamine (1.39 mL, 1.03 g, 8 mmol, 1 eq.), n-Bu_4NBr (1.30 g, 4 mmol, 0.50 eq.), and $Pd(OAc)_2$ (0.090 g, 0.4 mmol, 0.05 eq.) were dissolved in 3 mL toluene under argon atmosphere. The mixture was heated under reflux (105 °C) for 24 hours, before cooling to room temperature. Reaction mixture was extracted with $NH_4Cl_{sat,aq}$ solution and dichloromethane. The combined organic phased were washed with brine, dried over anhydrous MgSO4, and concentrated under reduced pressure to complete dryness. The resultant dark residue was purified by column chromatography (silica gel, hexane/ethylacetate, 2:1 v/v). ^{1}H NMR (400 MHz, $CDCl_3$) δ 7.82 ppm (d, J = 3.2 Hz, 2H), 7.37 ppm (d, J = 3.2 Hz, 2H). ^{13}C NMR (101 MHz, $CDCl_3$) δ 161.6 ppm, 143.9 ppm, 120.9 ppm.

Synthesis of 5,5'-Dibromo-2,2'-Bithiazole

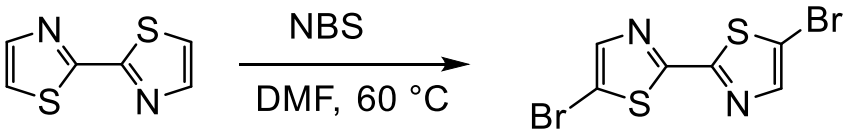

Scheme S3. Reaction scheme of 5,5'-dibromo-2,2'-bithiazole starting with 2,2'-bithiazole.

The synthesis 5,5'-dibromo-2,2'-bithiazole was carried out according to literature.[4]
2,2'-Bithiazole (1.00 g, 5.94 mmol, 1 eq.) was dissolved in 10 mL of diemthylformamide (DMF) and heated to 60 °C under argon. Subsequently, NBS (4.24 g, 23.76 mmol, 4 eq.) was added to the solution at once and the resulting mixture was stirred for 4 hours at 60 °C. The reaction mixture was then allowed to slowly cool down to r.t. during which time needle shaped crystals formed in solution. The crystals were collected by vacuum filtration, washed with cold methanol and dried in vacuo. ^{1}H NMR (400 MHz, $CDCl_3$) δ 7.77 ppm (s, 2H).

Synthesis of the polymer

Most polymers were synthesized according to the method described by A. Thomas et al.[5]. Detailed reaction parameters can be found in Table S1. EPT and Y were added in a molar ratio of 1:1.5 into a Schlenk flask and were dissolved in anhydrous DMF and diisopropylamine (DIA). The reaction mixture was heated to 100 °C under inert atmosphere. $Pd(PPh_3)_4$ and CuI were dissolved in 1 mL DMF in a Schlenk flask and added shortly after the reaction mixture reaches 100 °C. The color and turbidity changes started some minutes after adding $Pd(PPh_3)_4$ and CuI. The reaction mixture was heated for 3 days at 100 °C at inert atmosphere. Subsequent, the precipitate was filtered and washed with THF, $CHCl_3$, water, and methanol. Further purification was done by Soxhlet extraction for one day using THF and methanol. The powders were dried in a vacuum oven at 100 °C for 24 h. The colours of the obtained polymers can be seen in Figure S2.

Table S1. Summary of reaction conditions.

Entry	EPT (mmol)	Y[a] (mmol)	$Pd(PPh_3)_4$ (mmol)	CuI (mmol)	DIA (mL)	DMF (mL)	Yield (%)	S_{BET} ($m^2\ g^{-1}$)
NP-3a	0.533	0.799	0.052	0.059	34	32	89.5	447
NP-3b	0.540	0.810	0.052	0.053	6	60	94.3	468
NP-4a	0.546	0.819	0.052	0.057	34	32	101.2	600
NP-4b	0.541	0.819	0.052	0.055	6	60	93.6	536
NP-5a	0.525	0.787	0.053	0.055	34	32	97.7	532
NP-5b	0.529	0.793	0.052	0.053	6	60	104.2	590
NP-6a	0.531	0.796	0.052	0.053	34	32	92.4	517
NP-6b	0.546	0.819	0.053	0.054	6	60	101.7	545
SNP-3a	0.528	0.792	0.052	0.054	34	32	94.6	418
SNP-3b	0.529	0.794	0.053	0.053	6	60	100.2	425
SNP-4a	0.525	0.787	0.054	0.063	1	60	107.0	346
SNP-4b	0.556	0.835	0.054	0.052	6	60	92.7	210

[a] Y is defined as: 9,10-dibromoanthracene for NP-3, 2,5-Dibromopyridine for NP-4, 2,5-dibromopyrimidine for NP-5, 3,6-dibromopyridazine for NP-6, 4,7-dibromobenzo-[c]-1,2,5thiadiazole for SNP-3, and 5,5'-dibromo-2,2'-bithiazole for SNP-4.

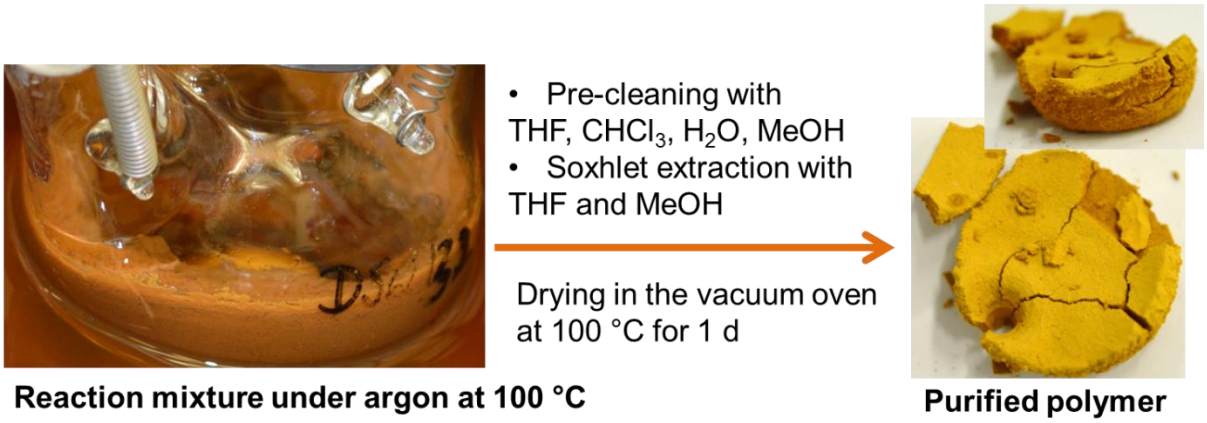

Figure S1. Purification of NP-6.

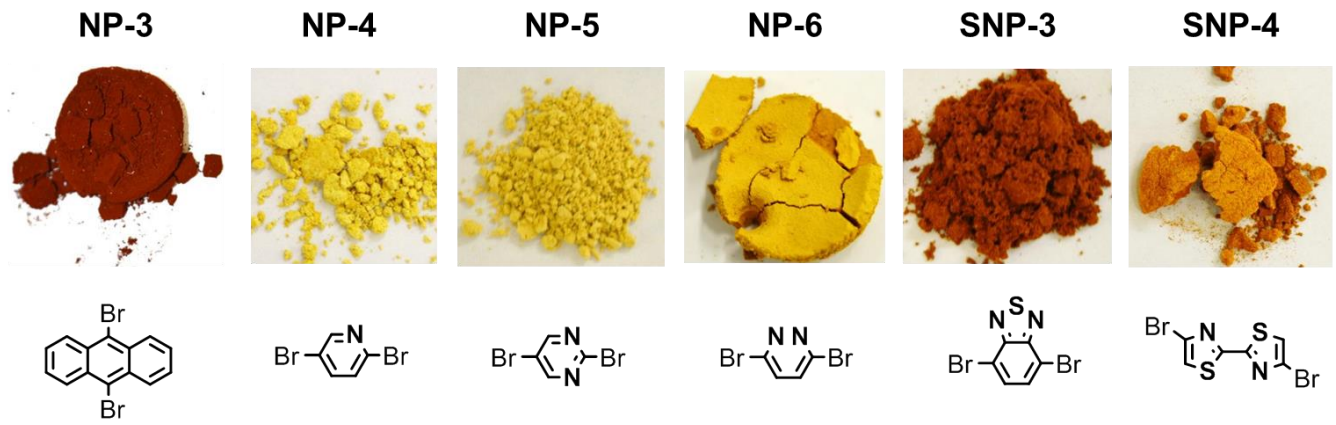

Figure S2. Overview of all synthesized polymers and the colour change of the polymer in dependence on the B2 tecton.

Results and Discussion

Elemental Analysis

Table S2. Elemental Analysis Data in weight % for the 6 samples: calculated white, found grey.

sample	C (%)	H (%)	N (%)	S (%)	C/N	Residue -(C, H, N)
NP-3	89.6	3.7	6.5	0	16:1	0
	81.8	3.8	6.0	0.11	16:1	8.4
NP-4	83.8	3.3	12.7	0	7.7:1	0
	75.7	3.5	11.2	0.11	7.9:1	9.6
NP-5	80.0	3.0	17.0	0	5.5:1	0
	71.4	3.5	15.5	0.09	5.4:1	9.6
NP-6	80.0	3.0	17.0	0	5.5:1	0
	72.4	4.0	15.1	0.08	6:1	8.5
SNP-3	74.7	2.6	14.3	8.3	6:1	0
	70.9	2.9	12.9	6.43	6.4:1	13.3
SNP-4	68.9	2.4	13.4	15.3	6:1	0
	64.7	2.7	12.5	14.84	6:1	20.1

Table S3. Elemental Analysis Data in weight percent and ICP-OES values for halogen and heavy metal ions trapped in the polymer matrix.

sample	C (%)	H (%)	N (%)	S (%)	Pd (%)	Cu (%)	Br (%)	I (%)	P (%)	Residue (%)
NP-3	89.6	3.7	6.5	0.00	0	0	0	0	0	0
	81.8	3.8	6.0	0.11	0.04	0.01	2.52	0.06	0.04	5.62
NP-4	83.8	3.3	12.7	0.00	0	0	0	0	0	0
	75.7	3.5	11.2	0.11	0.12	0.07	2.23	0.51	0.23	6.33
NP-5	80.0	3.0	17.0	0.00	0	0	0	0	0	0
	71.4	3.5	15.5	0.09	0.24	0.06	2.80	0.00	0.11	6.30
NP-6	80.0	3.0	17.0	0.00	0	0	0	0	0	0
	72.4	4.0	15.1	0.08	0.04	0.05	0.14	0.09	0.16	7.94
SNP-3	74.7	2.6	14.3	8.3	0	0	0	0	0	0
	70.9	2.9	12.9	6.43	0.06	0.07	0.86	0.12	0.15	5.61
SNP-4	68.9	2.4	13.4	15.3	0	0	0	0	0	0
	64.7	2.7	12.5	14.84	0.13	0.01	0.30	0.00	0.08	4.74

Transparent rows display the theoretical values, grey marked rows show the measured values; residue can be assigned as oxygen.

X-ray (EDX) Spectrum Analysis

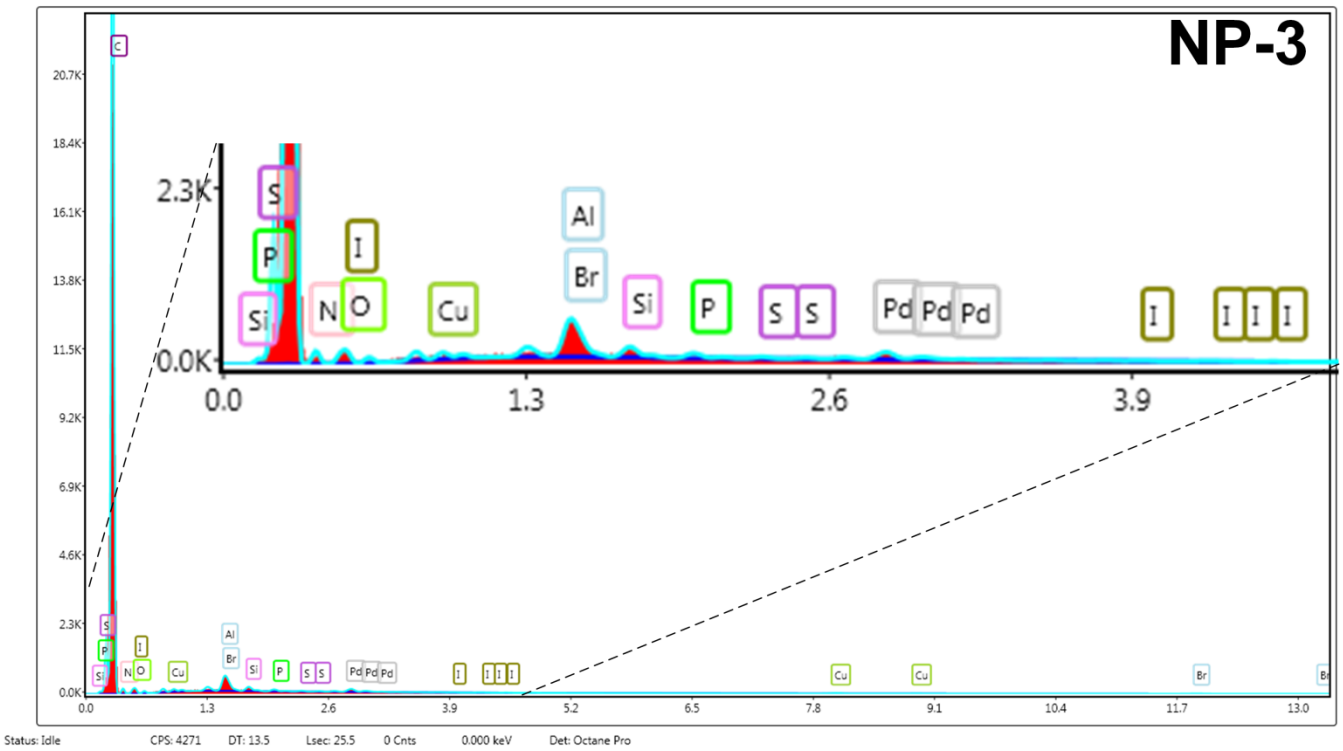

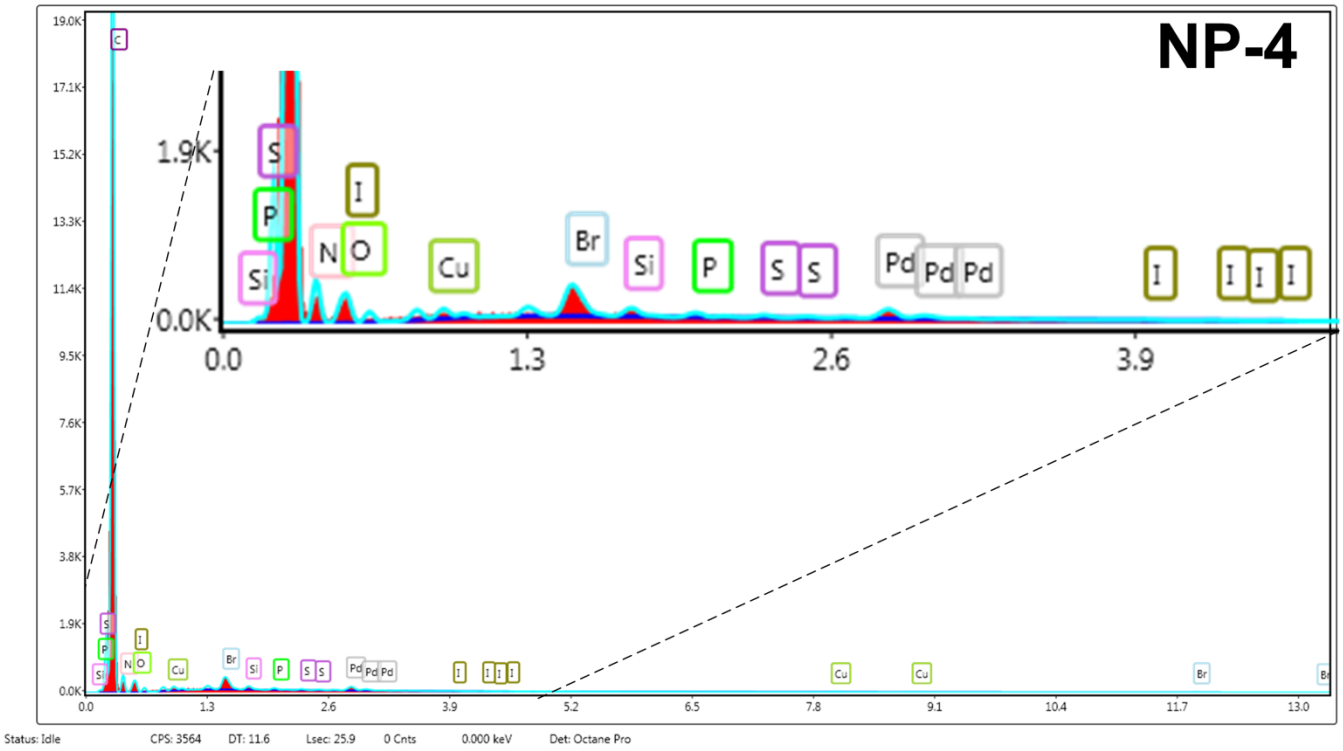

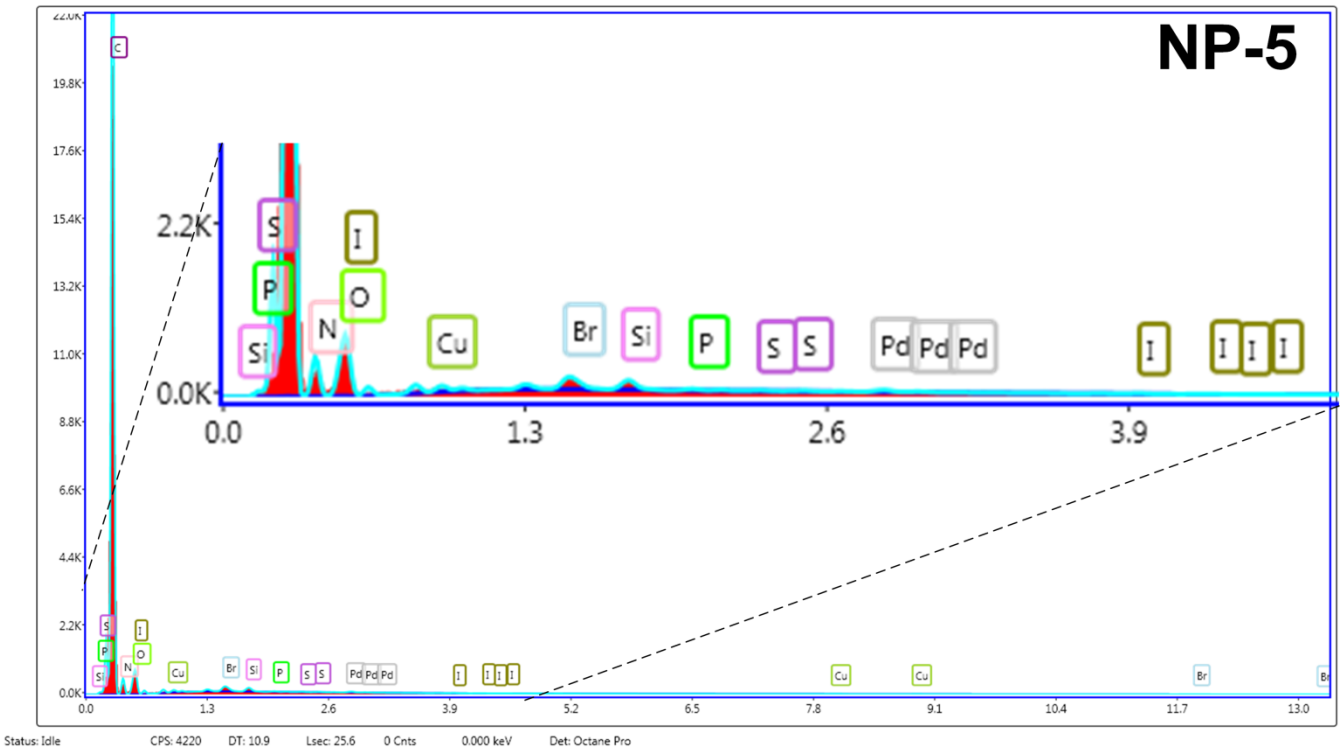
NP-5
2.2K
0.0K
0.0
1.3
2.6
3.9
C
S
P
Si
I
O
N
Cu
Br
Si
P
S S
Pd Pd Pd
I
I I I
Status: Idle
CPS: 4220
DT: 10.9
Lsec: 25.6
0 Cnts
0.000 keV
Det: Octane Pro

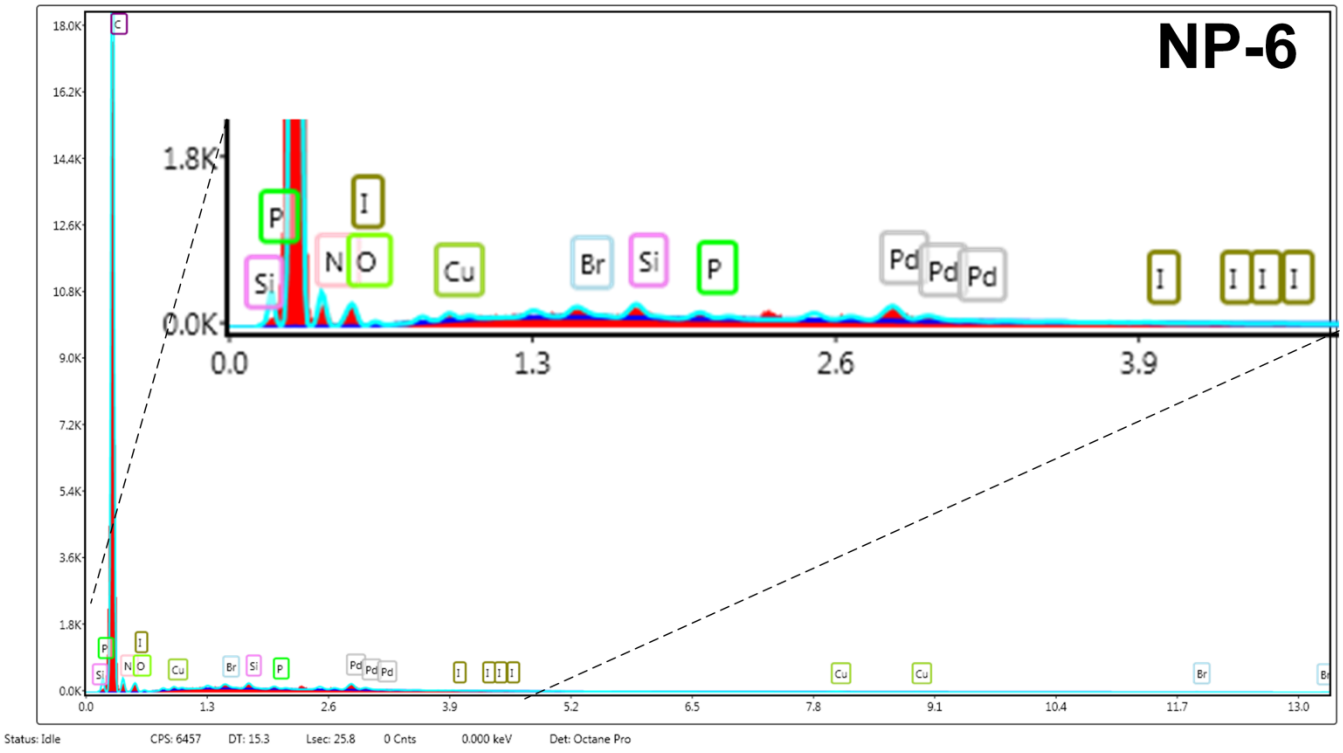
NP-6
1.8K
0.0K
0.0
1.3
2.6
3.9
C
P
Si
I
N O
Cu
Br
Si
P
Pd Pd Pd
I
I I I
Status: Idle
CPS: 6457
DT: 15.3
Lsec: 25.8
0 Cnts
0.000 keV
Det: Octane Pro

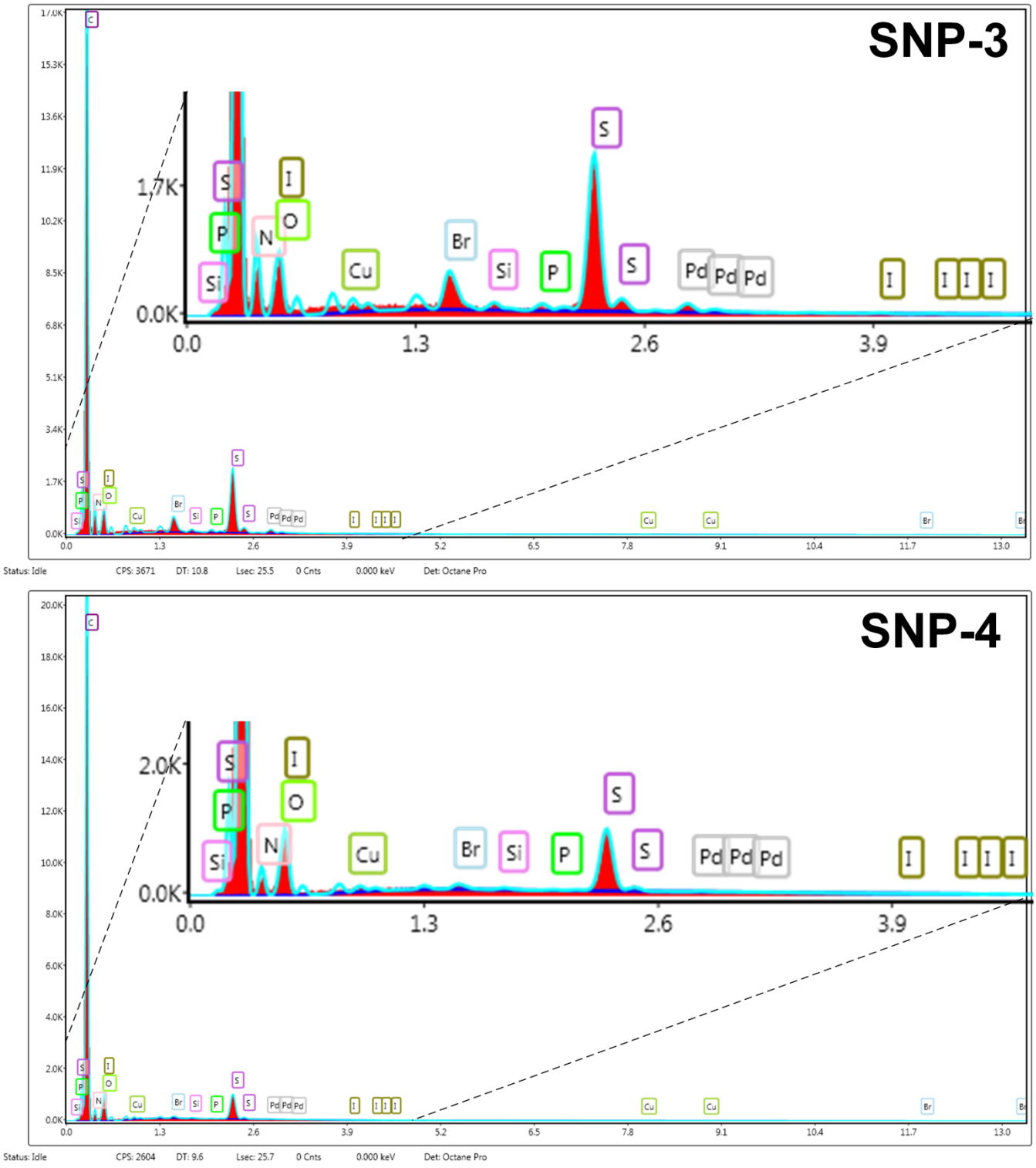

Figure S3. EDX spectra from SEM images.

Table S4. Elements detected by EDX in weight percent.

sample	C (%)	H (%)	N (%)	S (%)	O (%)	Pd (%)	Cu (%)	Br (%)	I (%)	P (%)
NP-3	89.6	3.7	6.5	0.00	0	0	0	0	0	0
	90.4	n.a.	4.31	0.05	2.43	0.21	0.15	1.88	0.06	0.14
NP-4	83.8	3.3	12.7	0.00	0	0	0	0	0	0
	71.83	n.a.	18.26	0.03	8.11	0.34	0.06	1.18	0.03	0.07
NP-5	80.0	3.0	17.0	0.00	0	0	0	0	0	0
	72.21	n.a.	16.36	0.04	10.52	0.17	0.12	0.07	0.02	0.07
NP-6	80.0	3.0	17.0	0.00	0	0	0	0	0	0
	72.39	n.a.	20.94	0.1	4.85	1.02	0.17	0.24	0.05	0.1
SNP-3	74.7	2.6	14.3	8.3	0	0	0	0	0	0
	66.54	n.a.	20.63	2.55	8.78	0.34	0.08	0.82	0.06	0.1
SNP-4	68.9	2.4	13.4	15.3	0	0	0	0	0	0
	73.74	n.a.	13.12	5.09	6.89	0.43	0.12	0.32	0.09	0.11

transparent rows display the theoretical values, grey marked rows show the measured values.

TGA

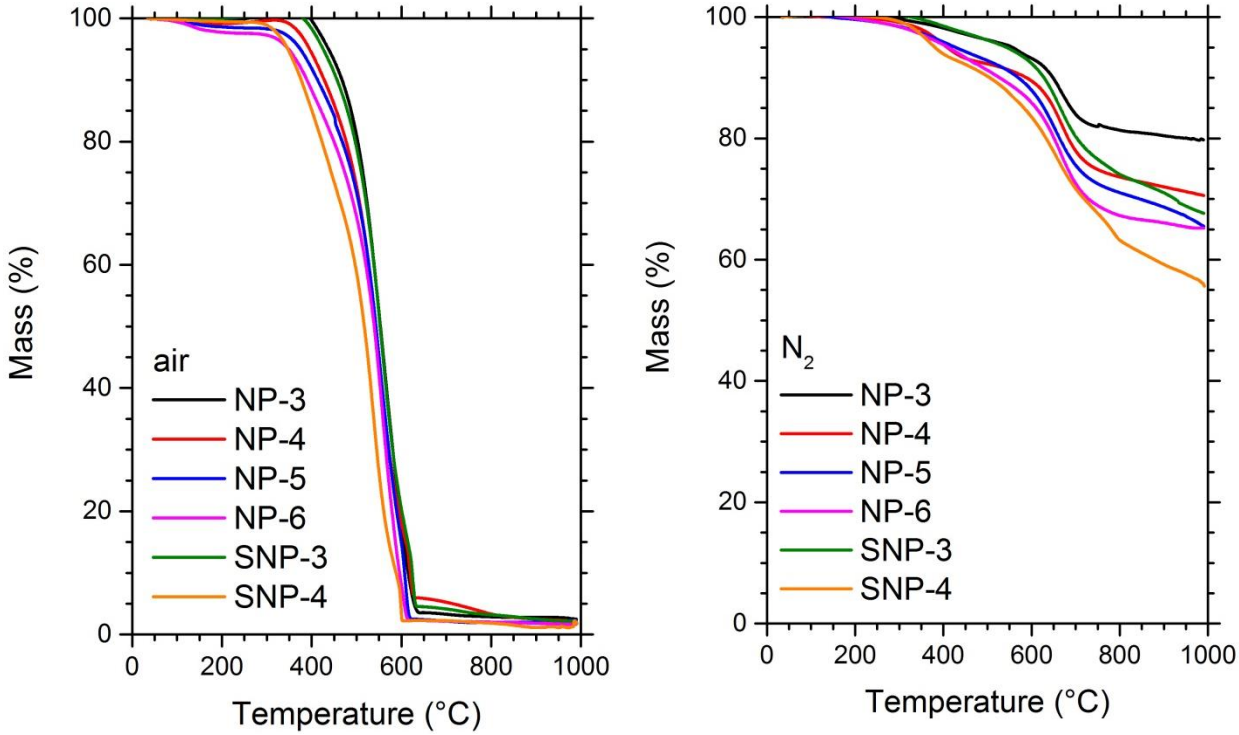

Figure S4. TGA data NP-3 (in black), NP-4 (in red), NP-5 (in blue), NP-6 (in magenta), SNP-3 (in green), SNP-4 (in orange) heated under air (*left-hand-side*) and heated under N_2 atmosphere (*right-hand-side*).

Comparison EA, EDX, and TGA

Table S5. comparison of the residual mass besides the known elements C, H, N, and S; O (oxygen) in EA and EDX can be due to moisture in the pores of the samples but it can also appear due to PdO or CuO. The difference should be represented by the comparison of the TGA values, as they should be related with the remaining PdO and CuO content within the error of measurement. However, the obtained values for Pd and Cu do not really match with the residue measured by TGA.

sample	EA[a]	EA[a](O, %)	EDX[b]	EDX[b](O, %)	TGA[c]
NP-3	8.4	2.78	4.92	2.34	2.5
NP-4	9.6	3.27	9.82	8.11	2.2
NP-5	9.6	3.30	11.01	10.52	2.3
NP-6	8.5	0.56	6.53	4.85	1.6
SNP-3	13.3	7.69	10.18	8.78	2.1
SNP-4	20.1	15.36	7.96	6.89	1.8

[a]calculated from Table S3, [b]calculated from ratio of elements in EDX spectra, see Table S4; [c]calculated from TGA Figure S5 at 1000 °C, heated under air conditions, s. Figure S5.

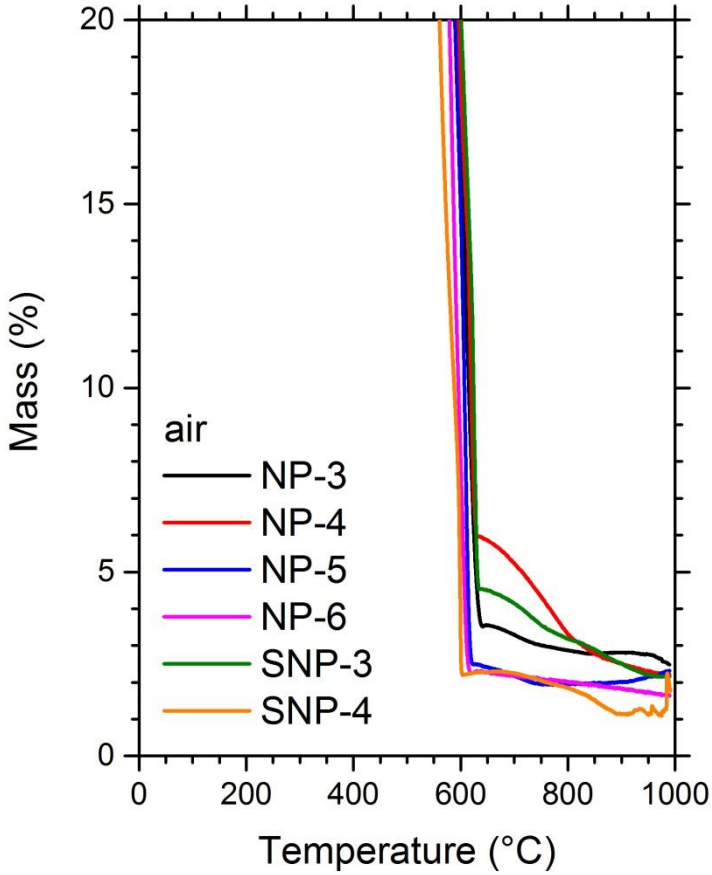

Figure S5. TGA NP-3 (in black), NP-4 (in red), NP-5 (in blue), NP-6 (in magenta), SNP-3 (in green), SNP-4 (in orange) with a magnification of the last 10 wt% from Figure S4 to see the residual mass at 1000 °C and its variations within the region of 600 and 1000 °C.

Powder X-ray Diffraction (XRD) Analysis

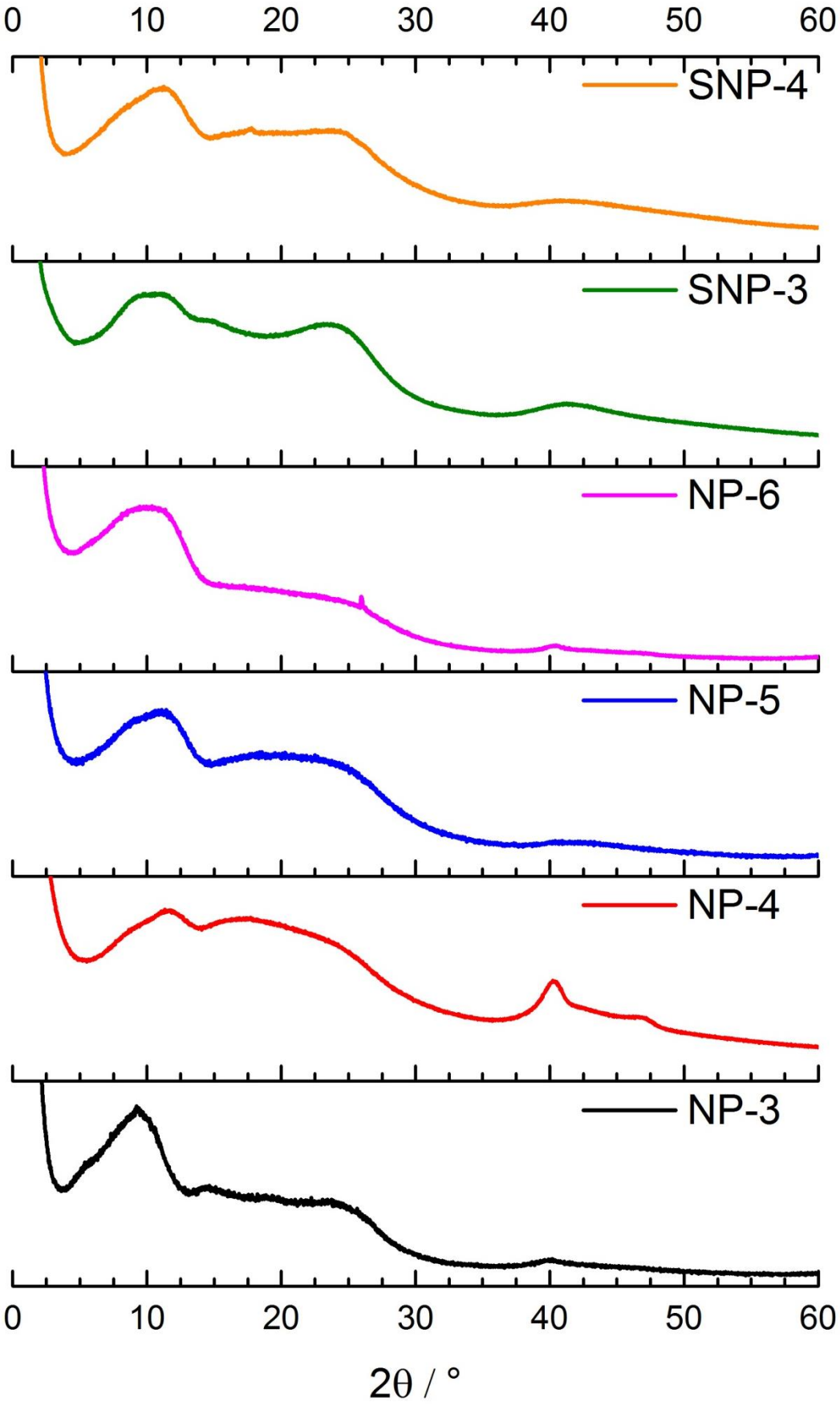

Figure S6. PXRD patterns NP-3 (in black), NP-4 (in red), NP-5 (in blue), NP-6 (in magenta), SNP-3 (in green), SNP-4 (in orange) in the range of 10 to 60°.

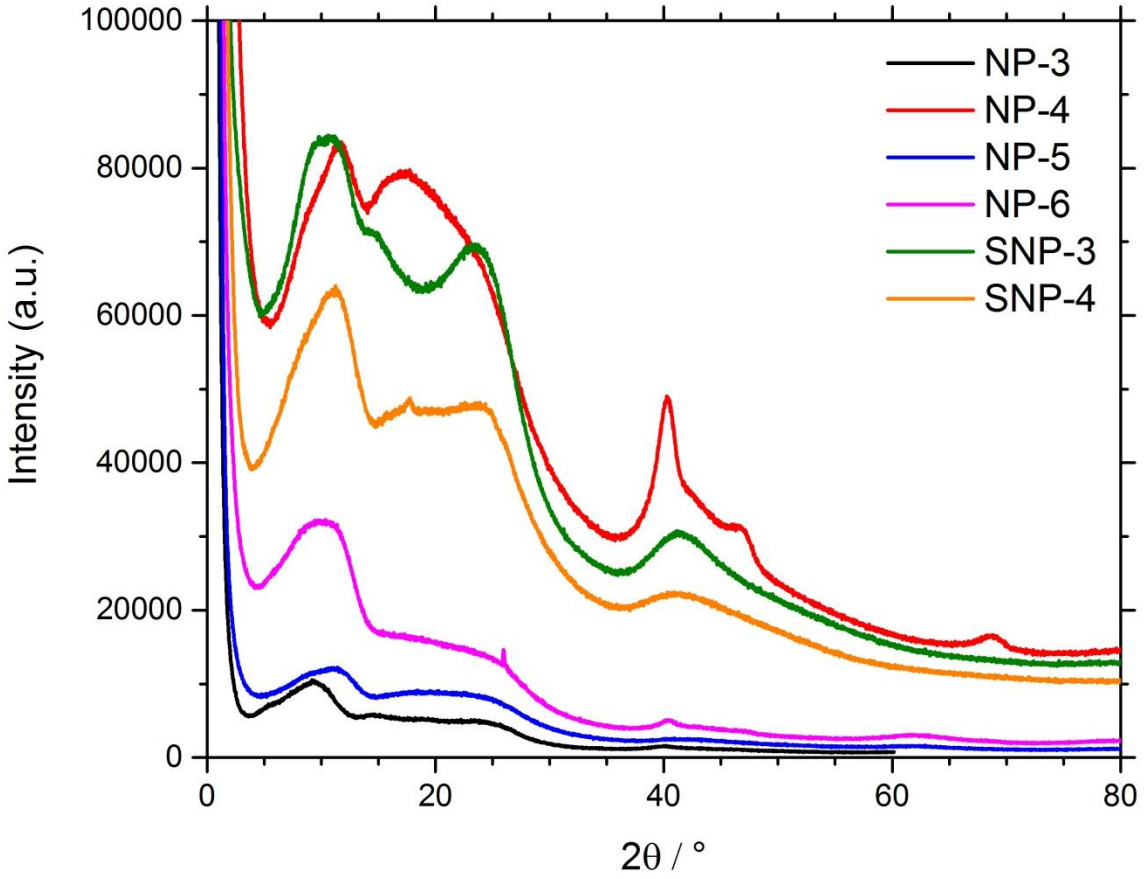

Figure S7. PXRD patterns NP-3 (in black), NP-4 (in red), NP-5 (in blue), NP-6 (in magenta), SNP-3 (in green), SNP-4 (in orange) in the range of 10 to 80°.

FT-IR

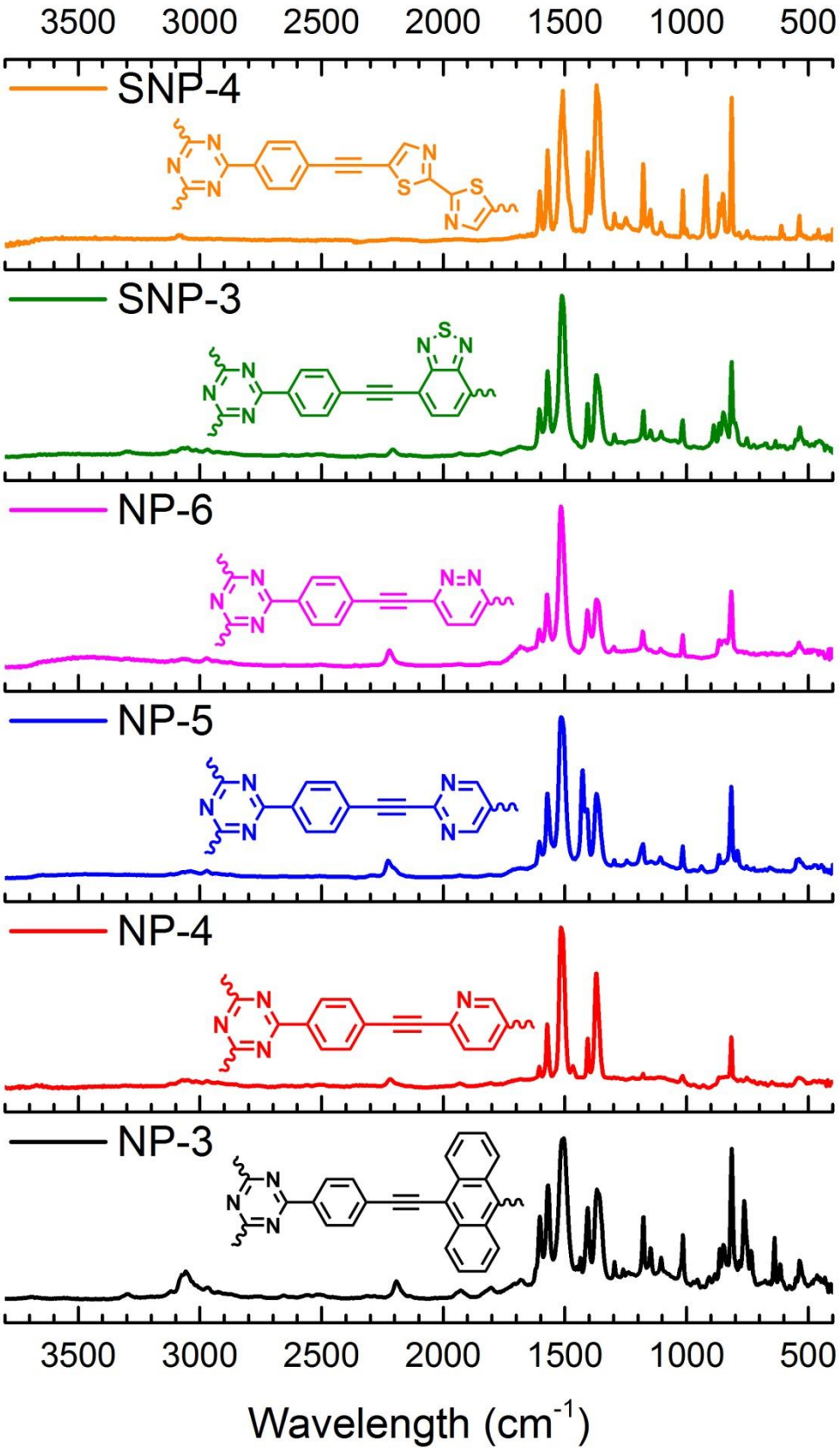

Figure S8. KBr-IR spectra NP-3 (in black), NP-4 (in red), NP-5 (in blue), NP-6 (in magenta), SNP-3 (in green), SNP-4 (in orange).

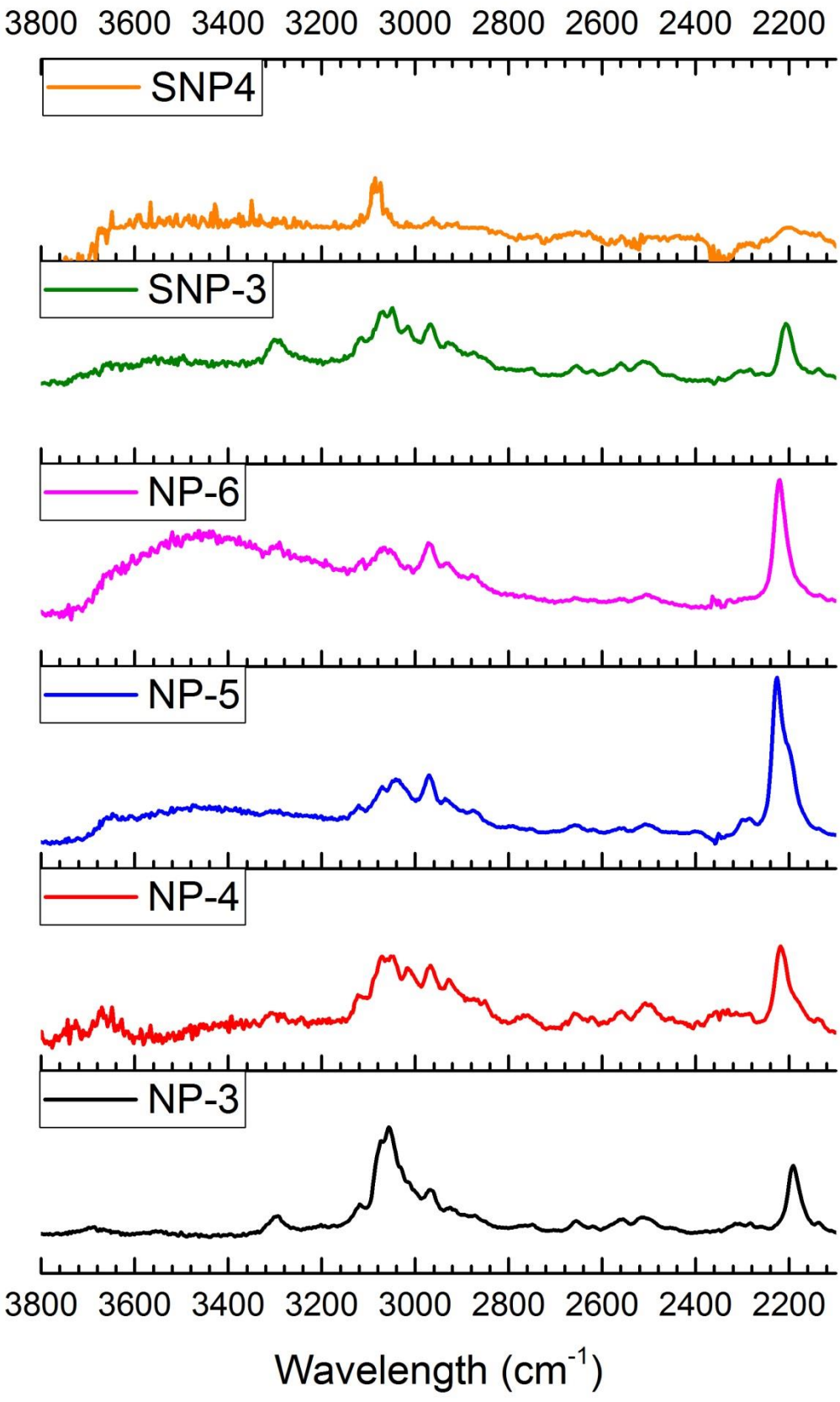

Figure S9. FT-IR spectra of NP-3 (in black), NP-4 (in red), NP-5 (in blue), NP-6 (in magenta), SNP-3 (in green), SNP-4 (in orange) at high wavelengths, featuring the characteristic terminal -C≡C-H triple bond vibration peak at 3300 cm^{-1} arising from unreacted end groups. The new formed -C≡C- exhibits a stronger intensity at around 2200 cm^{-1}.

UV-Vis with band gap calculations

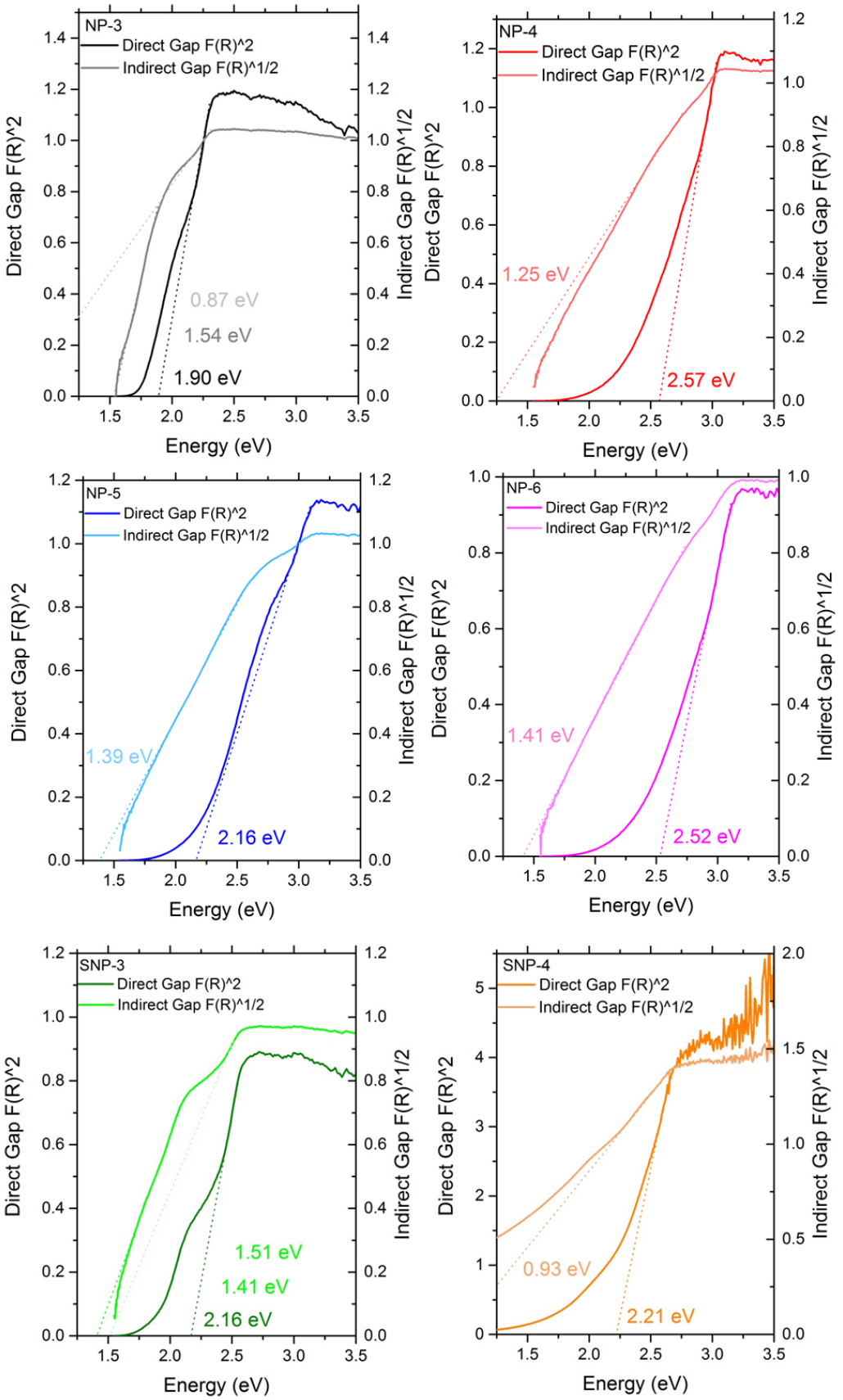

Figure S10. Solid-state UV/Vis diffuse-reflectance spectra with direct and indirect band gap calculations.

Pore Size Distribution

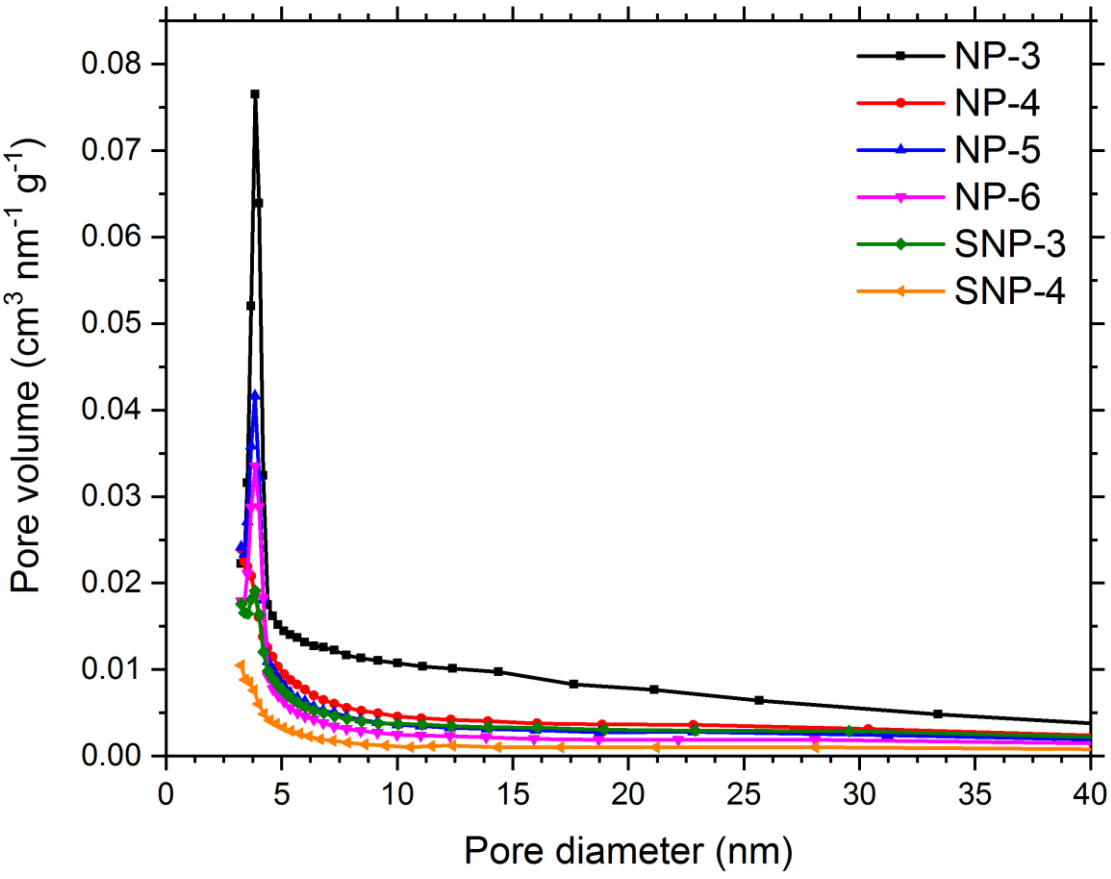

Figure S11. Pore size distributions calculated from desorption isotherms with BJH for NP-3 (in black), NP-4 (in red), NP-5 (in blue), NP-6 (in magenta), SNP-3 (in green), SNP-4 (in orange).

Theoretical calculations

Periodic DFT calculations. First, initial structure of SNPs and NPs single layer periodic cells were constructed in Virtual Nano Lab (VNL) graphical environment of QuantumWise and optimised at the PBE/DZP/GD2/5x5x16k-points level using the atomistix toolkit (ATK) of QuantumWise.[6] This yielded nicely flat layer structures. Each of these was then subjected to optimization with unconstrained Bravais lattice parameters at PBE/DZP/GD2/5x5x16k-points level with increased density mesh cut-off of 250 Ha. We then calculated the band structure, density of states etc. at the level mentioned above. The molecular structure and frontier orbital Bloch states were then visualised in VNL.

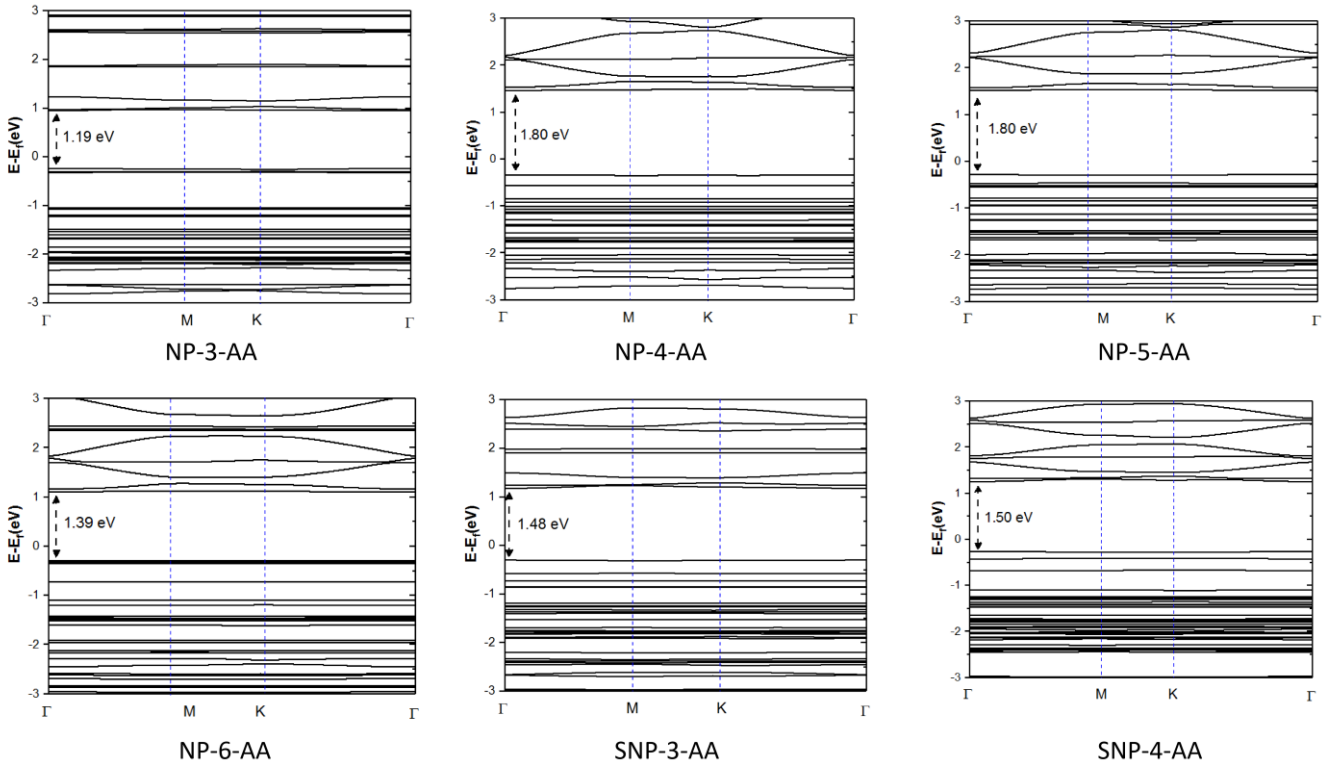

Figure S12. Band structures of SNPs NPs based on single layer periodic cells. The Fermi levels are set to zero.

Computational details

The DFT calculations were performed using the projector augmented wave (PAW)[7] formalism within the generalized gradient approximation (GGA) method with Perdew-Burke-Ernzerhof (PBE) exchange-correlation functional as implemented in Vienna Ab Initio Simulation Package (VASP).[8], [9], [10] The cutoff energy of 800 eV for the plane-wave basis set has been consistently used in all calculations. The convergence criterion of 0.01 was used for the forces in geometry optimizations and 10^{-5} eV was used for the energy convergence. The lattice parameters and atomic positions were fully relaxed. The Brillouin zone for structure optimizations was sampled with the Monkhorst-Pack[11] special *k*-point mesh on 1×1×3. D3 dispersion correction was adopted in all calculations.[12]

All geometry optimizations were performed with the unit cell consisting of one layer of COF, starting from the geometry described as AA eclipsed. Final structures are depicted in Figure S13 and cif files are attached in SI.

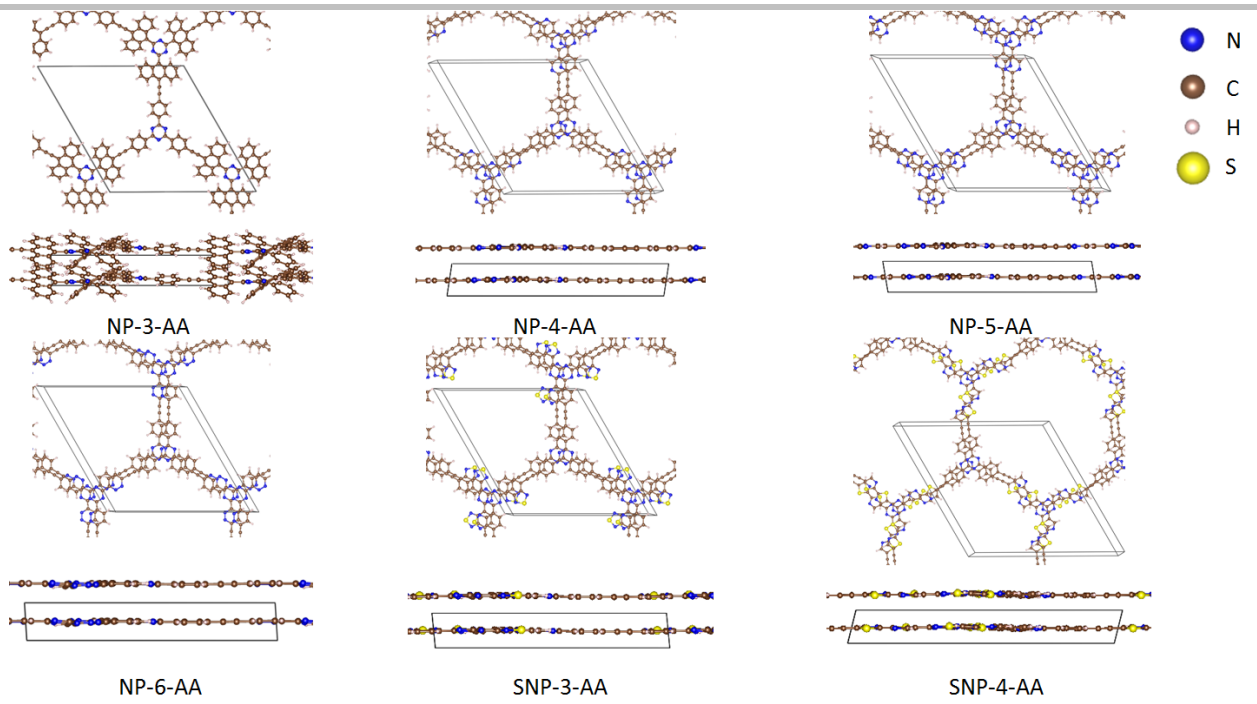

Figure S13. The top and side views of each optimised structure.

XPS

X-ray photoelectron spectroscopy (XPS) spectra were recorded on an AXIS ULTRA (Kratos Analytical, England). For the measurement, a Mono-Al $K_{\alpha 1,2}$ X-ray-source was used with a rated input of the x-ray tube of 300 W at 20 mA. The analyzer had a pass energy of 160 eV (overview spectra), and 20 eV (high resolution spectra), respectively. For charge compensation a low energy electron source in contact with a magnetic immersion lens was used.
In general, all compounds exhibit a N 1s peak at 399 eV which corresponds to the nitrogen in the triazine ring.[13] Model compounds 2,2'-Biquinoline and 2,2':6,2''-Terpyrine, which both contain sp2 nitrogen within an aromatic ring feature similar N 1s signals.[14] Phenyl possesses a common peak at around 284,76 eV for conjugated C-atoms (=^{Ph}C–^{Ph}C=^{Ph}C–). C-atoms in the triazine ring feature a slight shift towards higher binding energies (around 286 eV) due to the –I effect of the nitrogen atoms.[15, 16]

Table S6. Elemental distribution and peak positions showing oxygen (O) and small amounts of palladium (Pd) in addition to carbon (C) and nitrogen (N) measured by XPS for NP-3.

Name	Peak BE	FWHM (eV)	Area (P) CPS eV	Atomic ratio (%)	Q
C1s	284.1	1.41	290777.2	90.13	1
N1s	398.09	1.37	28990.65	5.79	1
O1s	532.21	3.07	31424.02	4.03	1
Pd3d	336.97	2.34	3365.13	0.06	1

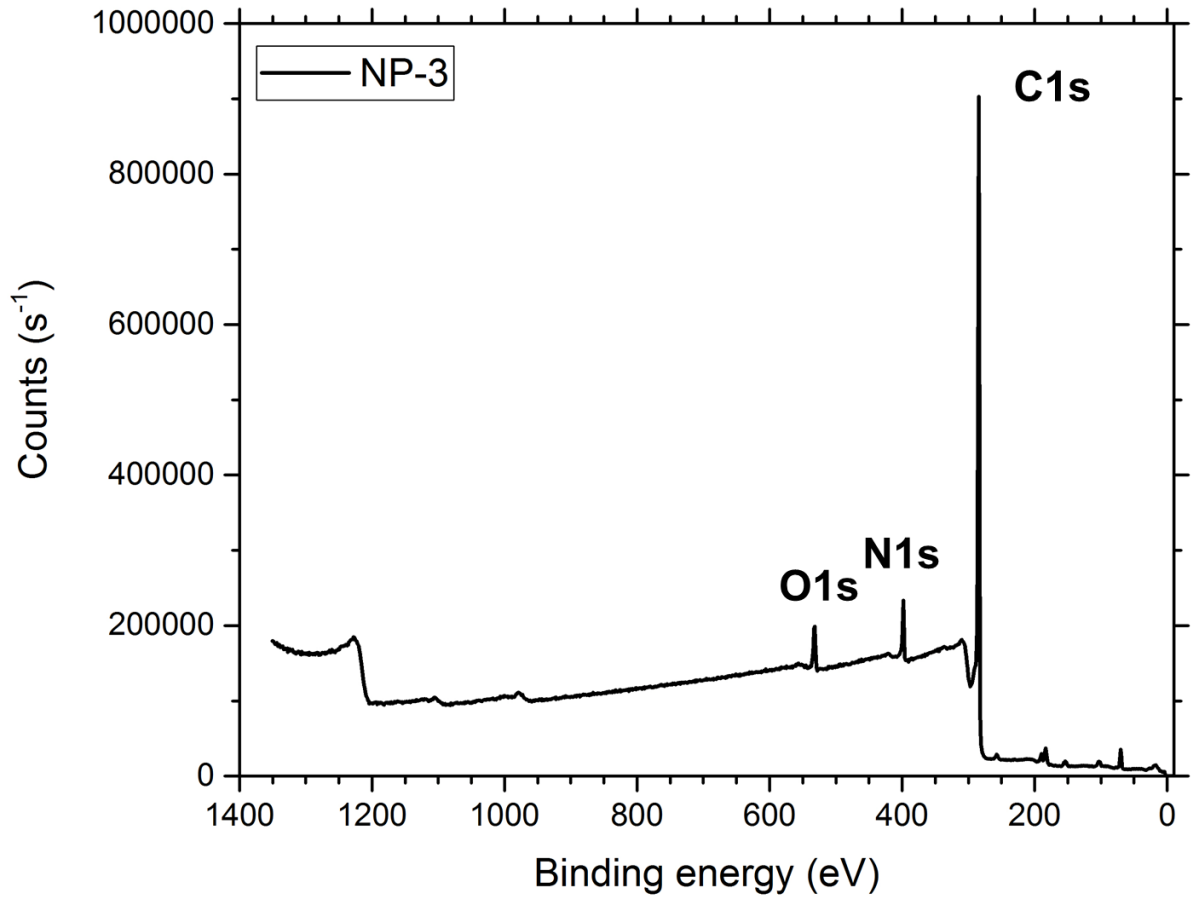

Figure S14. Survey spectrum showing oxygen (O) in addition to the expected elements carbon (C) and nitrogen (N) measured by XPS for NP-3.

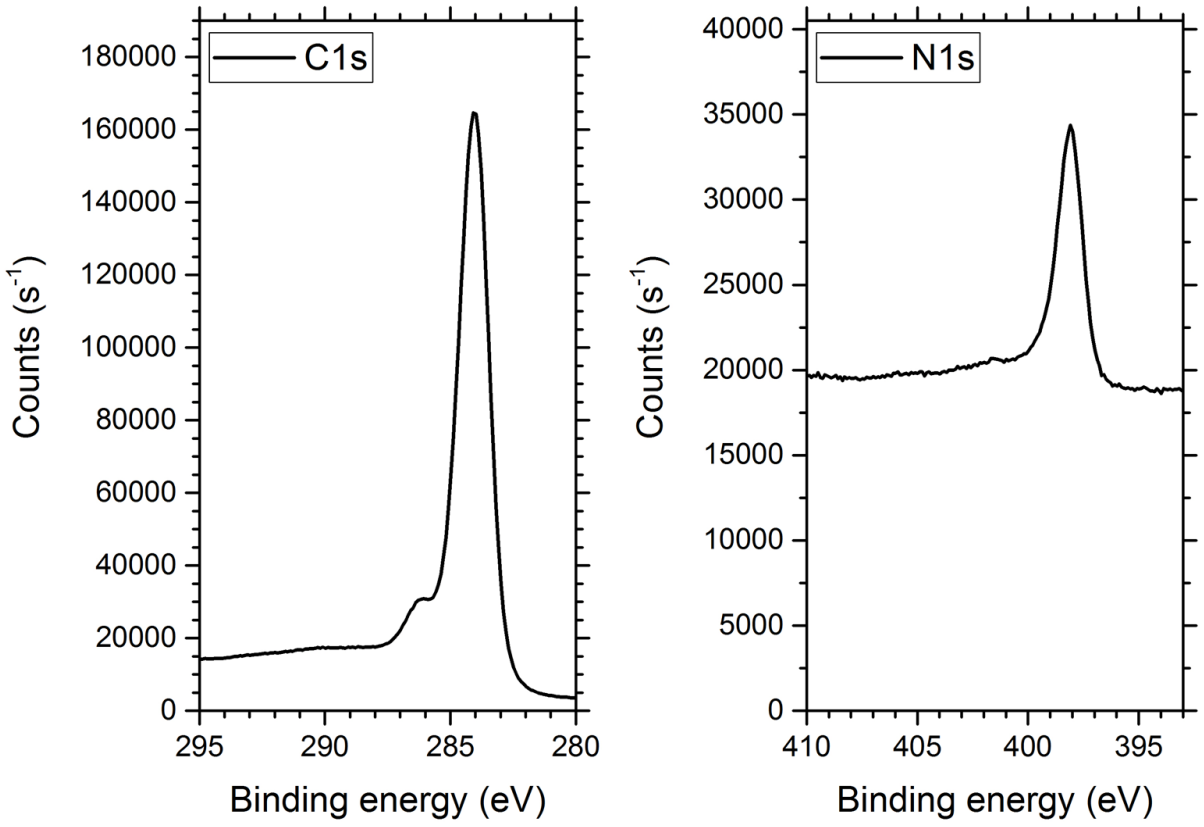

Figure S15. XPS peaks of 1Cs and 1Ns for NP-3.

Table S7. Elemental distribution and peak positions showing oxygen (O) and small amounts of palladium (Pd) and copper (Cu) in addition to carbon (C) and nitrogen (N) measured by XPS for NP-4.

Name	Peak BE	FWHM (eV)	Area (P) CPS eV	Atomic ratio (%)	Q
C1s	284.36	1.55	343559	84.9	1
Cu2p	947.14	0.23	2293.64	0.04	1
N1s	398.42	1.34	66053.49	10.51	1
O1s	531.9	2.83	43306.13	4.43	1
Pd3d	337.11	1.59	8731.29	0.12	1

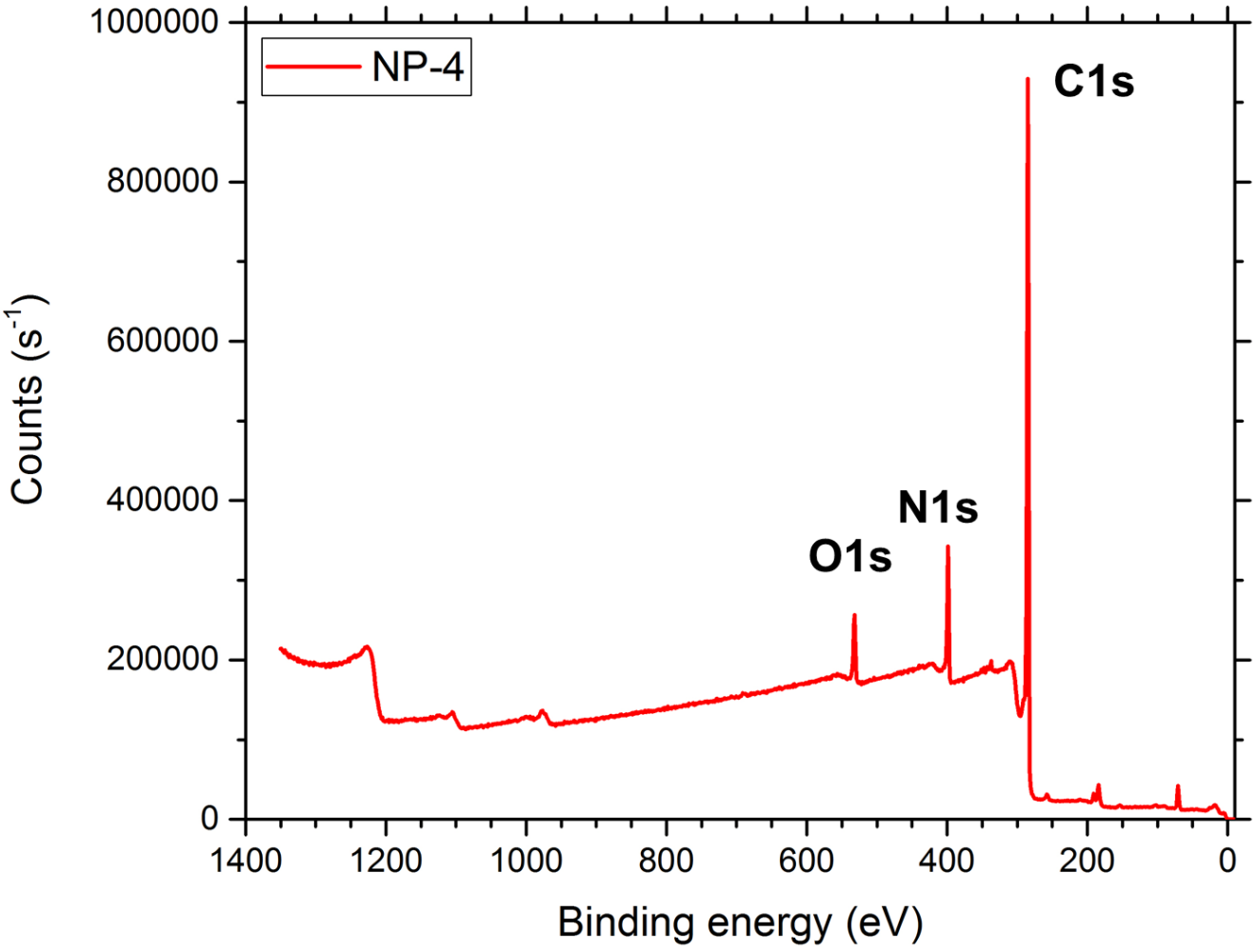

Figure S16. Survey spectrum showing oxygen (O) in addition to the expected elements carbon (C) and nitrogen (N) measured by XPS for NP-4.

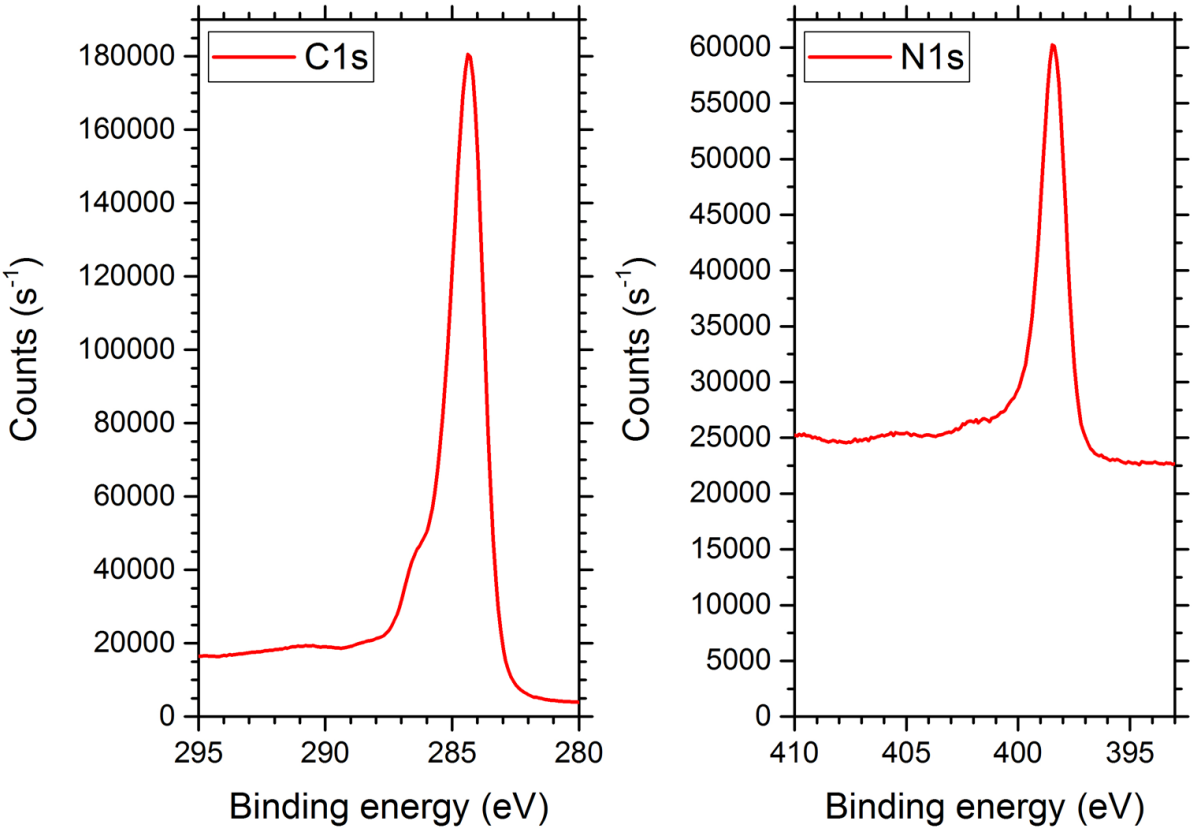

Figure S17. XPS peaks of 1Cs and 1Ns for NP-4.

Table S8. Elemental distribution and peak positions showing oxygen (O) and small amounts of palladium (Pd) and copper (Cu) in addition to carbon (C) and nitrogen (N) measured by XPS for NP-5.

Name	Peak BE	FWHM (eV)	Area (P) CPS eV	Atomic ratio (%)	Q
C1s	284.37	1.62	260720.4	80.71	1
Cu2p	932.19	1.85	3671.05	0.08	1
N1s	398.58	1.55	69655.19	13.89	1
O1s	531.91	3.01	40301.34	5.16	1
Pd3d	337.28	0.75	9767.34	0.16	1

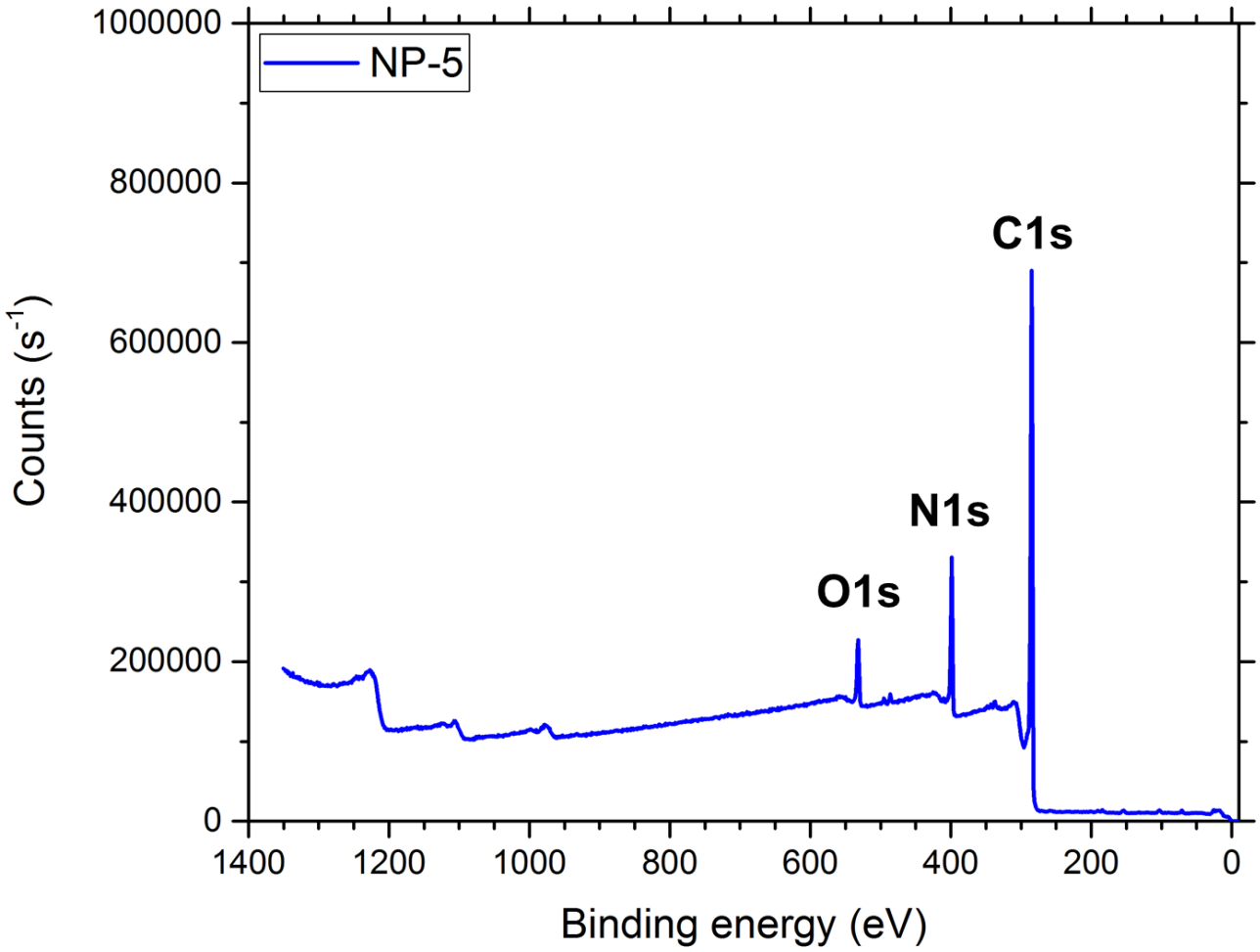

Figure S18. Survey spectrum showing oxygen (O) in addition to the expected elements carbon (C) and nitrogen (N) measured by XPS for NP-5.

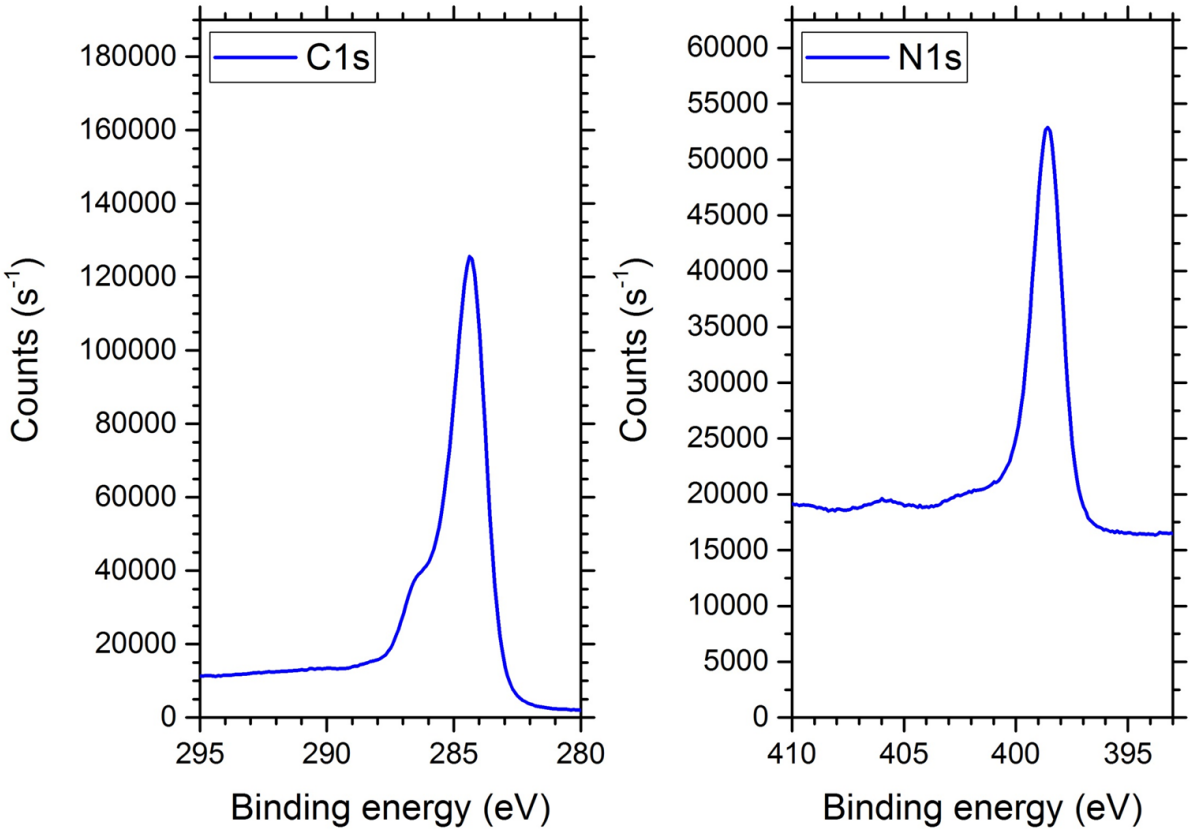

Figure S19. XPS peaks of 1Cs and 1Ns for NP-5.

Table S9. Elemental distribution and peak positions showing oxygen (O) and small amounts of palladium (Pd) and copper (Cu) in addition to carbon (C) and nitrogen (N) measured by XPS for NP-6.

Name	Peak BE	FWHM (eV)	Area (P) CPS eV	Atomic ratio (%)	Q
C1s	284.42	1.6	336679.5	85.17	1
Cu2p	936.53	0	3183.69	0.05	1
N1s	398.49	1.39	65761.35	10.71	1
O1s	532.05	2.98	37608.66	3.94	1
Pd3d	337.22	1.82	9015.11	0.12	1

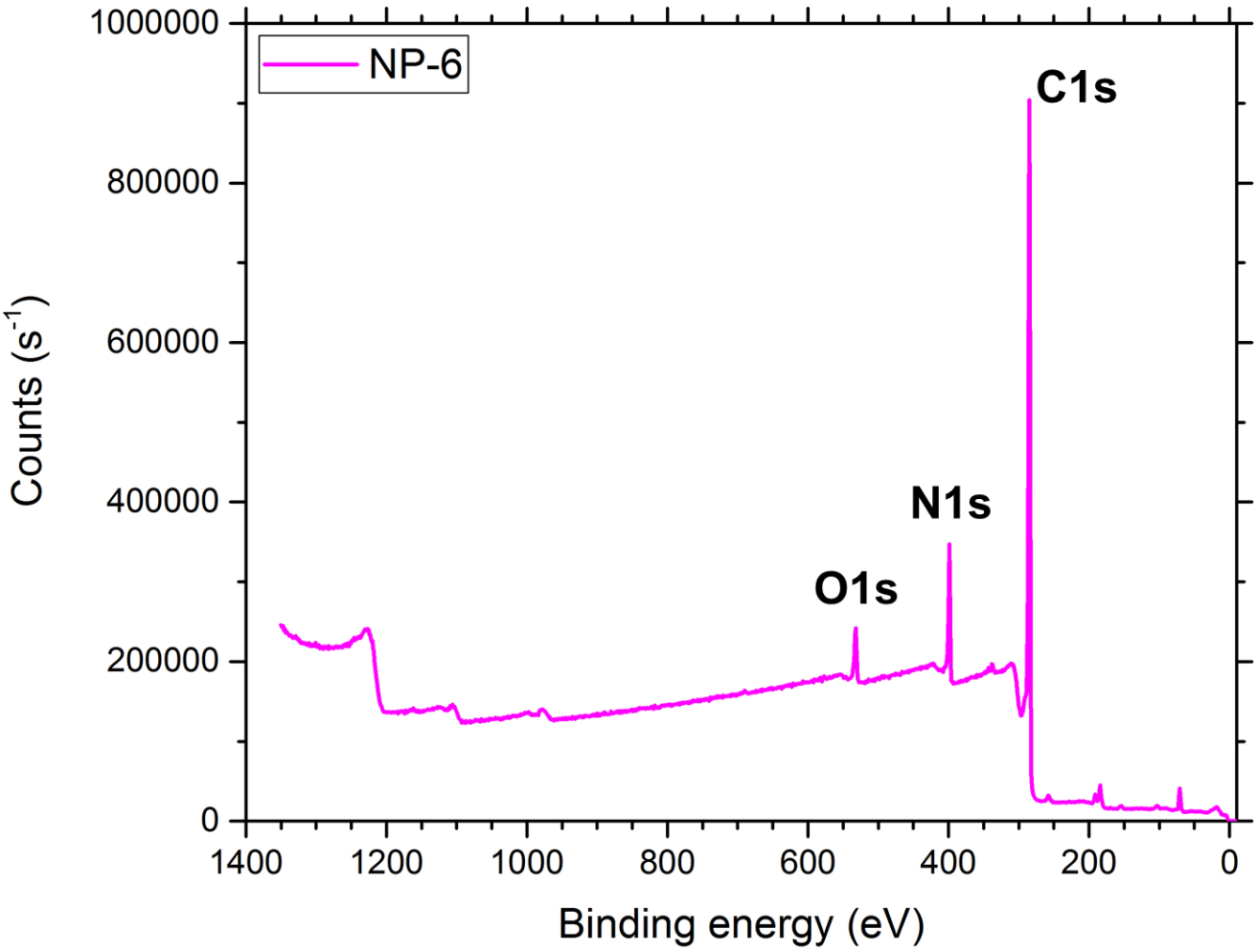

Figure S20. Survey spectrum showing oxygen (O) in addition to the expected elements carbon (C) and nitrogen (N) measured by XPS for NP-6.

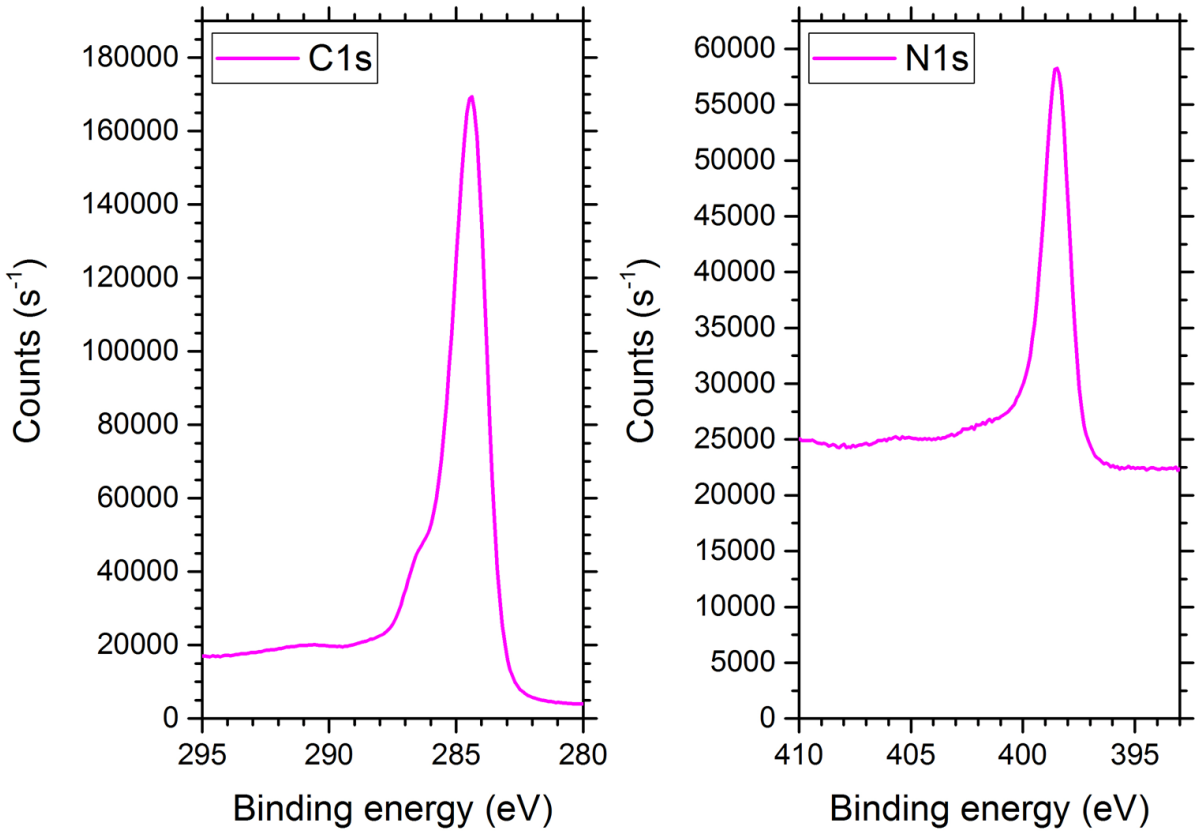

Figure S21. XPS peaks of 1Cs and 1Ns for NP-6.

Table S10. Elemental distribution and peak positions showing oxygen (O) and small amounts of palladium (Pd) in addition to carbon (C) and nitrogen (N) measured by XPS for SNP-3.

Name	Peak BE	FWHM (eV)	Area (P) CPS eV	Atomic ratio (%)	Q
C1s	284.34	1.63	238860.8	82.28	1
N1s	398.71	1.91	57366.21	12.73	1
S2p	165.02	1.32	18898.63	2.93	1
O1s	532.35	3.53	33691.19	4.8	1
Pd3d	337.36	1.69	9973.43	0.18	1

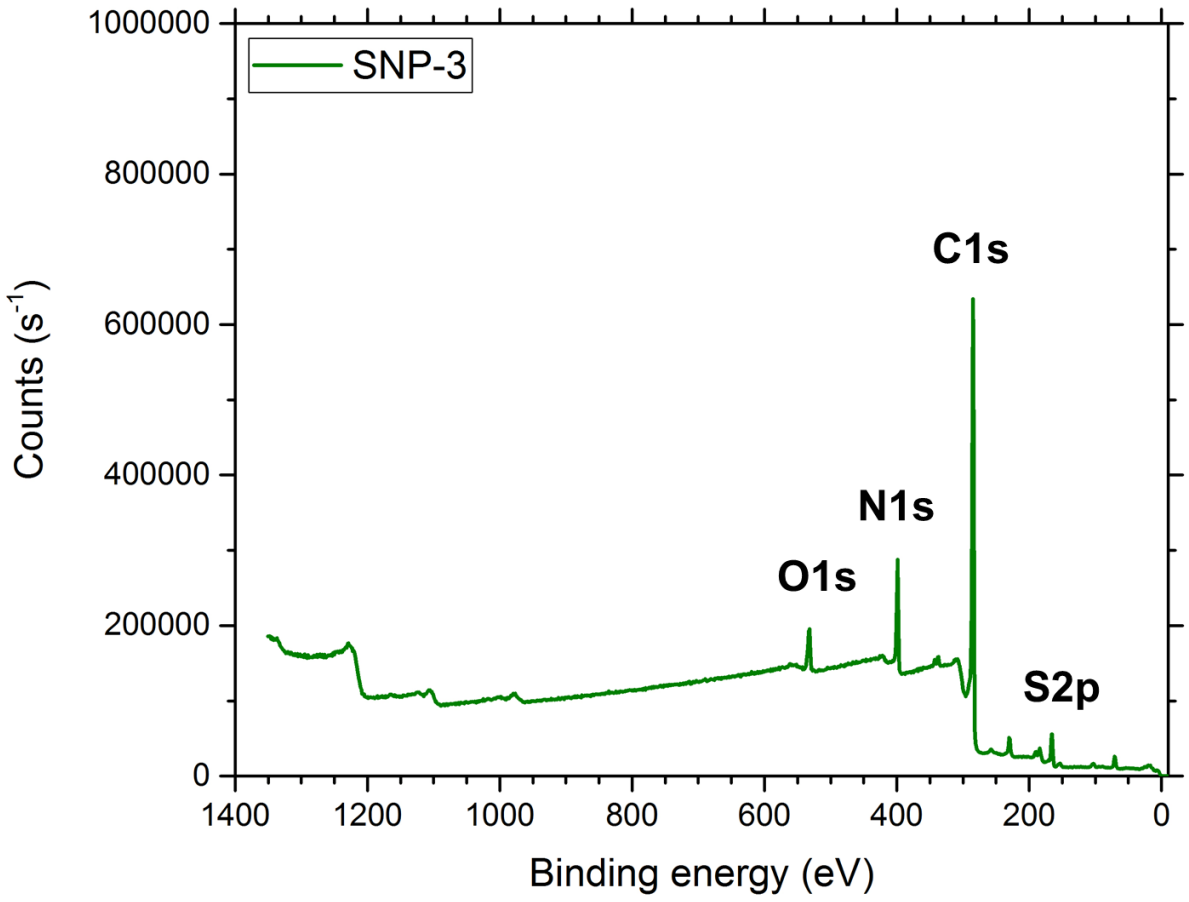

Figure S22. Survey spectrum showing oxygen (O) in addition to the expected elements carbon (C), nitrogen (N) and sulphur(S) measured by XPS for SNP-3.

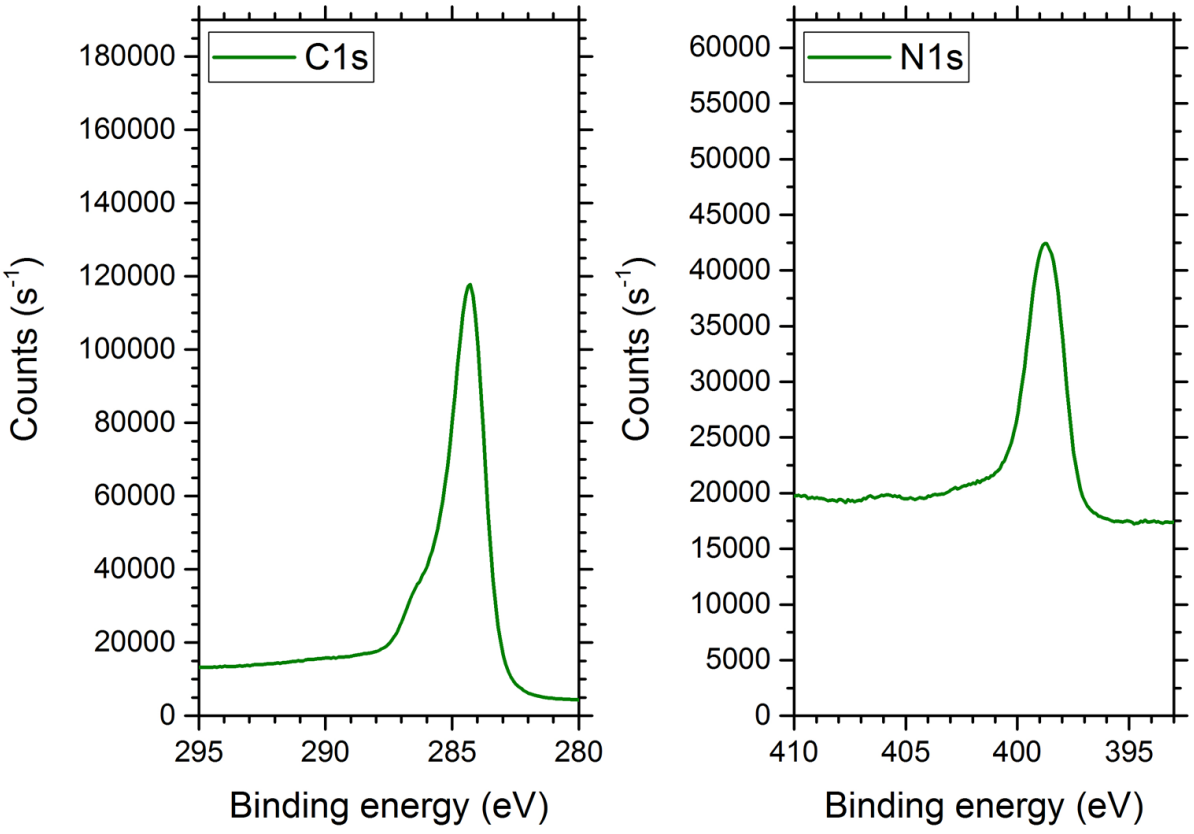

Figure S23. XPS peaks of 1Cs and 1Ns for SNP-3.

Table S11. Elemental distribution and peak positions showing oxygen (O) and small amounts of palladium (Pd) in addition to carbon (C) and nitrogen (N) measured by XPS for SNP-4.

Name	Peak BE	FWHM (eV)	Area (P) CPS eV	Atomic ratio (%)	Q
C1s	284.43	1.64	296639.8	81.3	1
N1s	398.51	1.27	76247.42	13.46	1
S2p	163.93	1.26	39993.53	6.78	1
O1s	532.21	3.14	41954.87	4.76	1
Pd3d	334.96	1.79	33259.72	0.49	1

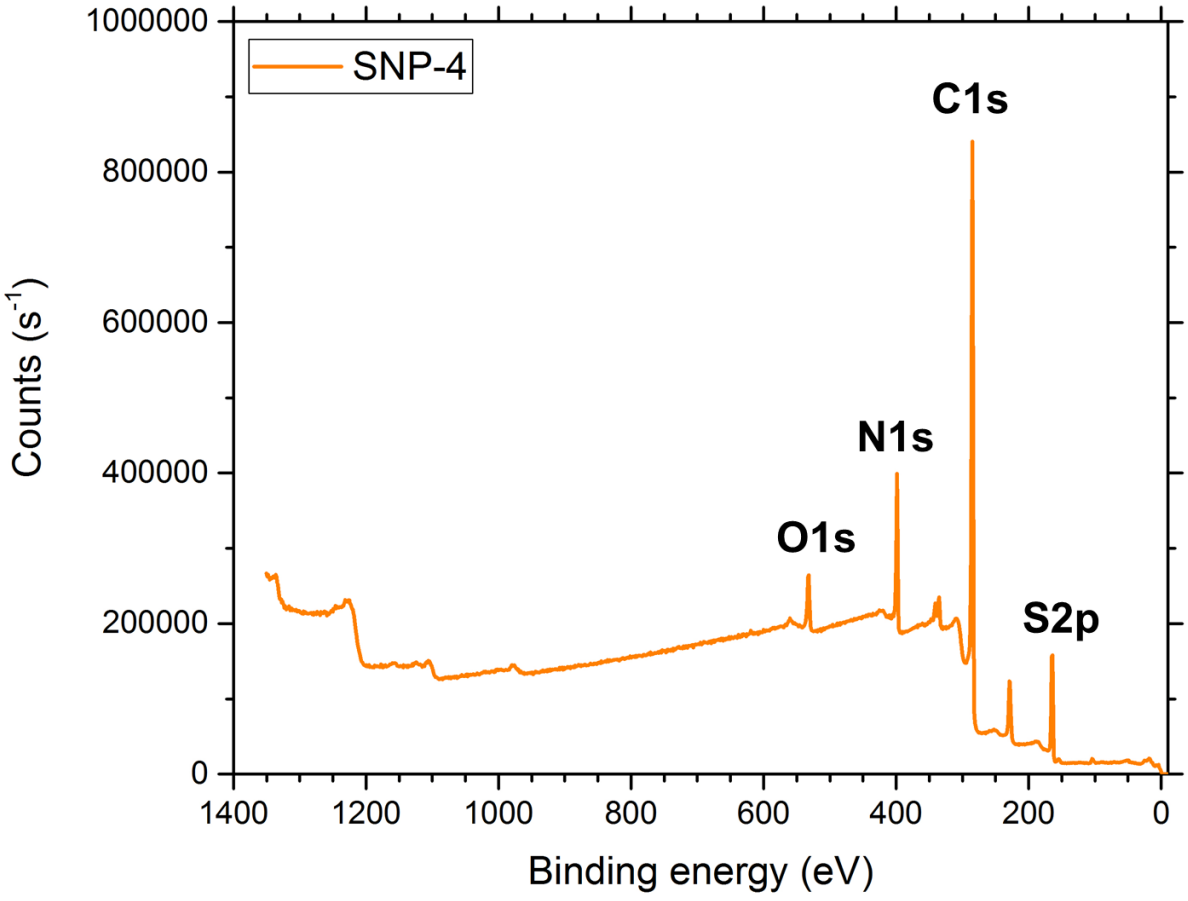

Figure S24. Survey spectrum showing oxygen (O) in addition to the expected elements carbon (C), nitrogen (N) and sulphur(S) measured by XPS for SNP-4.

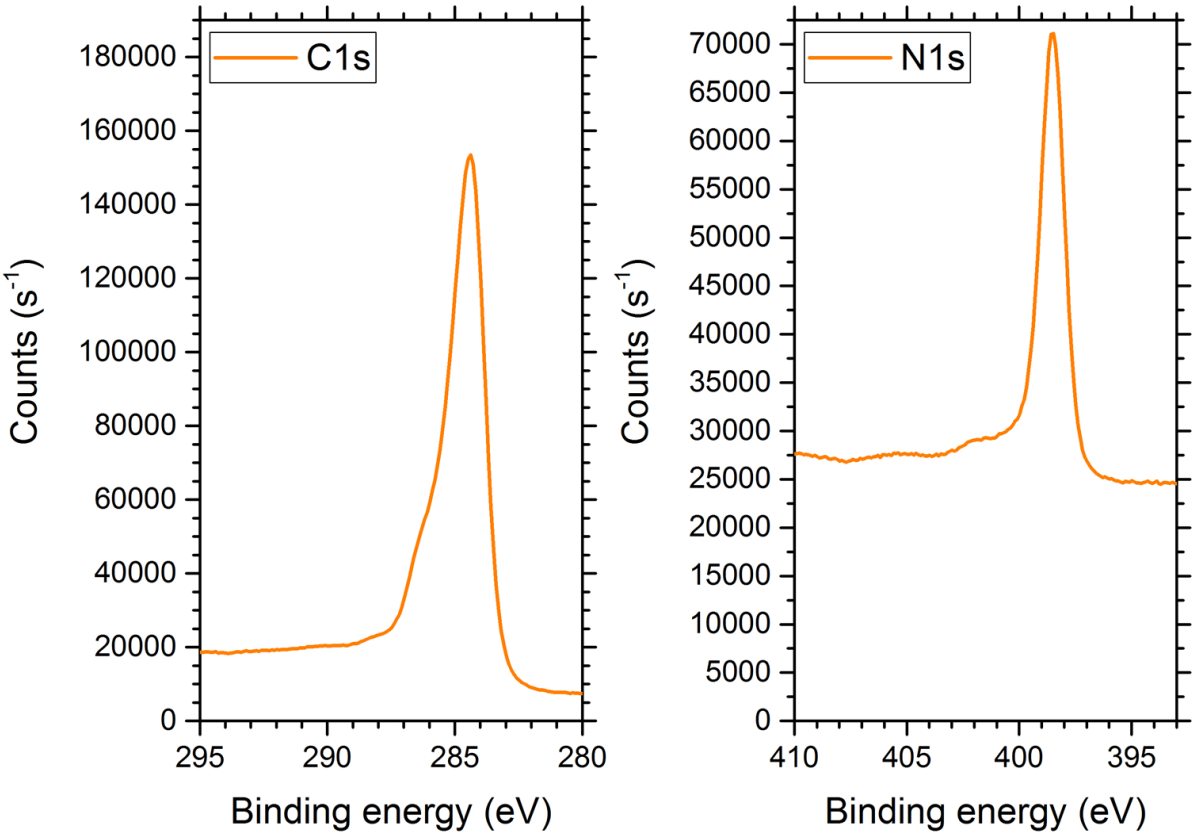

Figure S25. XPS peaks of 1Cs and 1Ns for SNP-4.

Photocatalytic hydrogen evolution experiments

Photocatalytic hydrogen evolution experiments were carried out in a jacketed 3-neck quartz reactor (Fig S25) with a total volume of 36 ml. 10 mg of catalyst was dispersed in 18 mL water:acetonitrile mixture (1:1) and 2 mL TEOA. 3wt% Pt(H_2PtCl_6) was added for the photodeposition of Pt co-catalyst. The reactor was closed using rubber septa, completely evacuated and purged with argon to remove any air and then irradiated with a 300 W Xe lamp (L.O.T.-Quantum design) equipped with a cut off filter of 395 nm. Headspace volume was calculated to be 16 mL.

During catalytic reactions, the temperature was kept fixed at 20 °C using a thermostat. Distance between the reactor and light source was also kept fixed at 10 cm and stirring speed was maintained at 600 rpm. Gas samples from the head space were taken after 15 h of reaction and were analysed by GC equipped with a TCD detector.

A control experiment with the same solvent mix and 3wt% Pt(H_2PtCl_6) but no additional polymer did not show any hydrogen evolved.

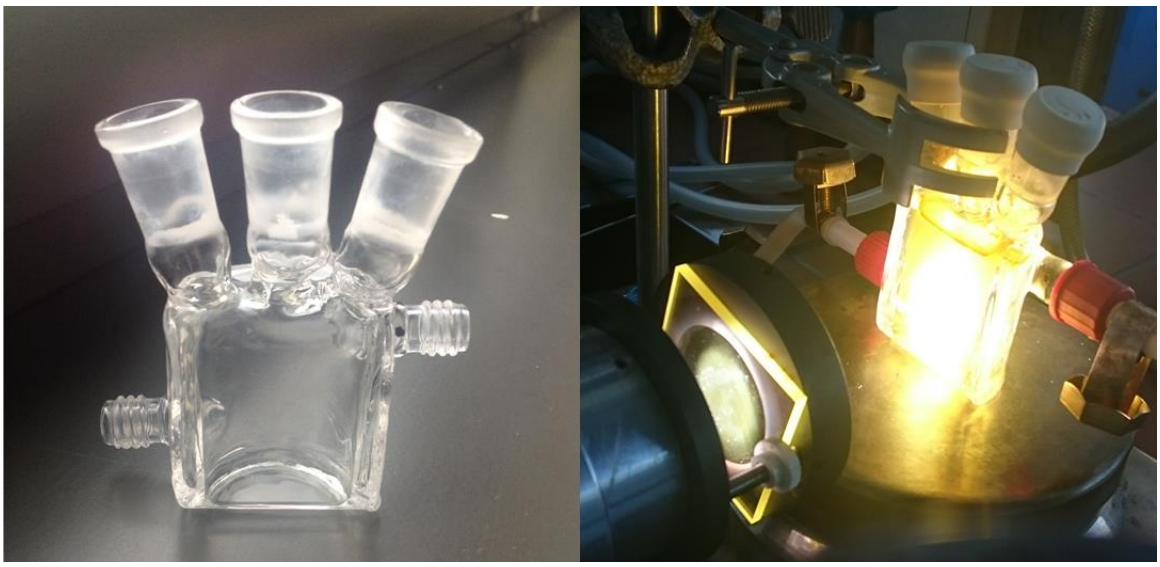

Figure S26. Photos of the reactor (left) catalytic reaction setup (right).

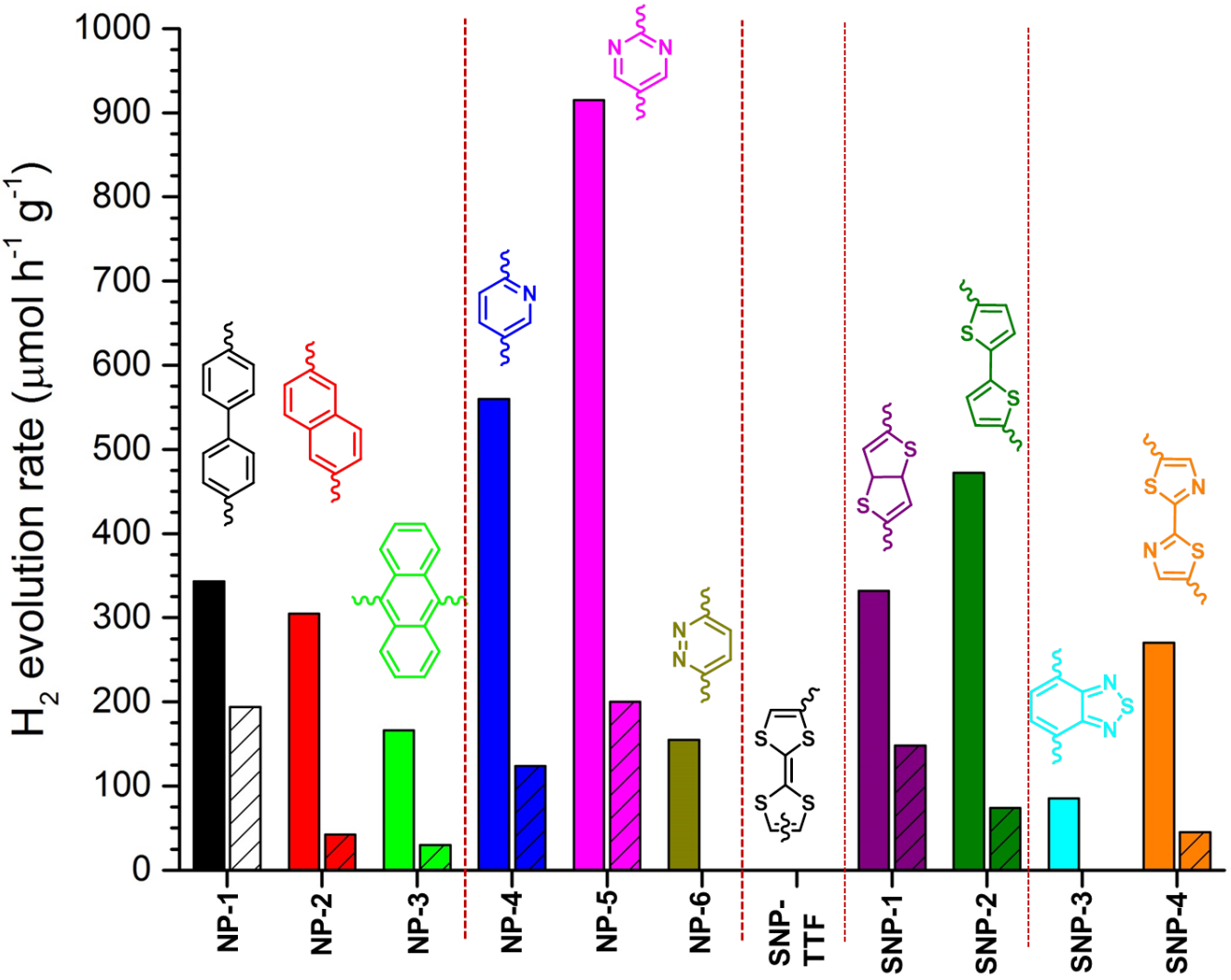

Figure S26. Hydrogen evolution rates of NPs, NNPs and SNPs in dependence of the monomer used as a linker. Striped bar indicates that no Pt co-catalyst was added. NP-1, NP-2, SNP-TTF, SNP-1, and SNP-2 were taken for comparison from the following reference.[17]

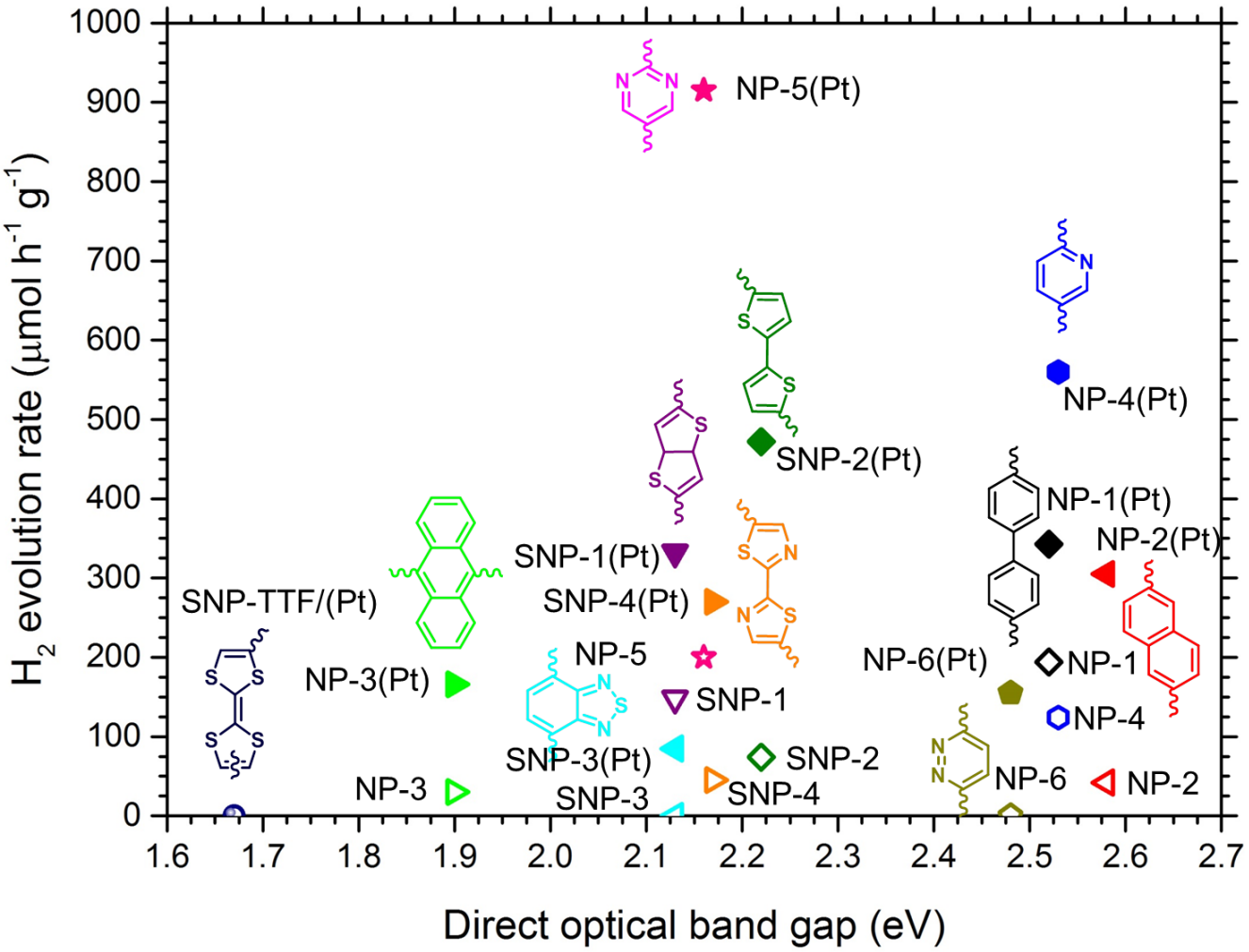

Figure S27. Hydrogen evolution rates of NPs, NNPs and SNPs in dependence of the direct band gap (calculated from UV/vis spectra). NP-1, NP-2, SNP-TTF, SNP-1, and SNP-2 were taken for comparison from the following reference. [17]

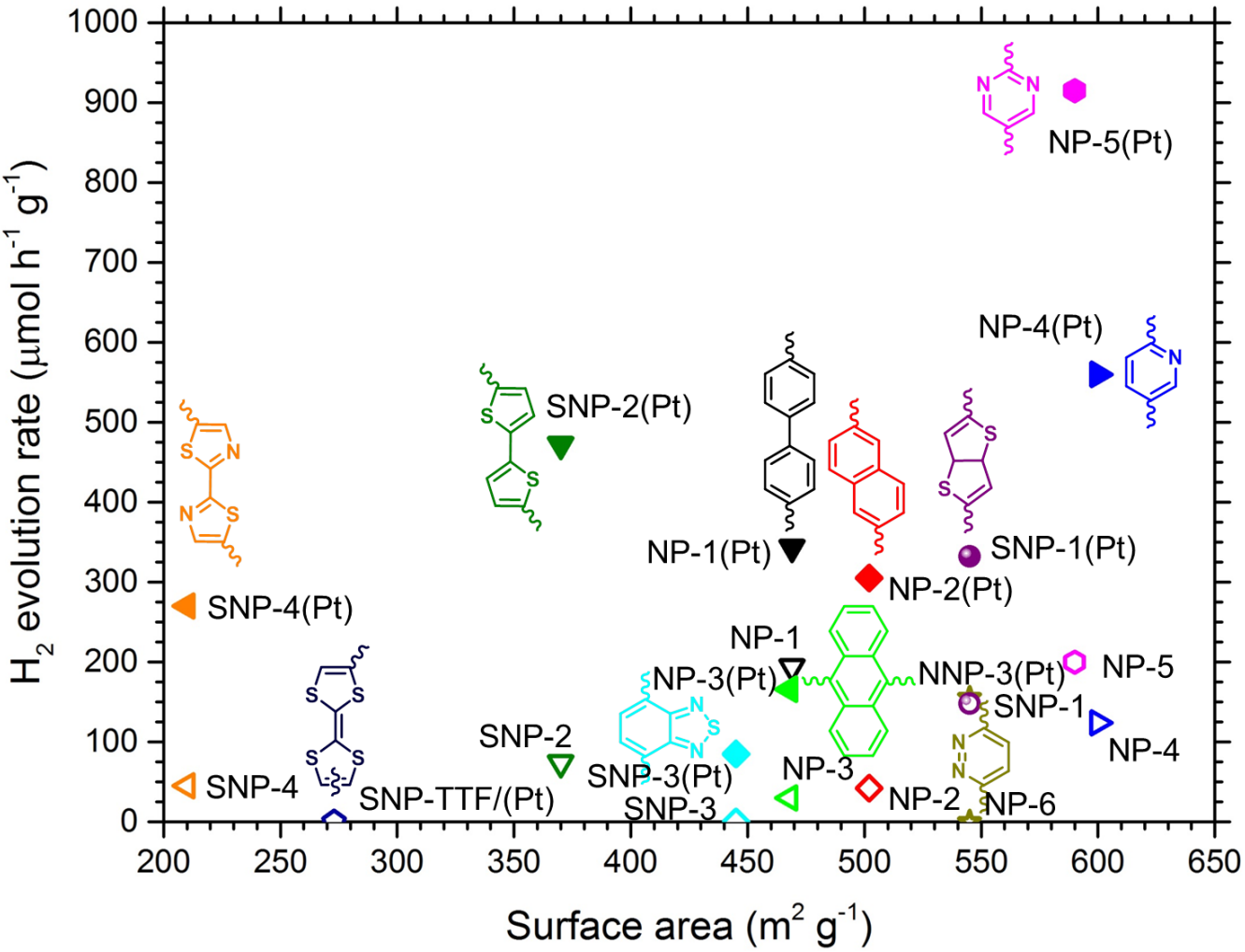

Figure S28. Hydrogen evolution rates of NPs, NNPs and SNPs in dependence of the surface area (calculated from N_2 sorption isotherms with BET). NP-1, NP-2, SNP-TTF, SNP-1, and SNP-2 were taken for comparison from the following reference. [17]

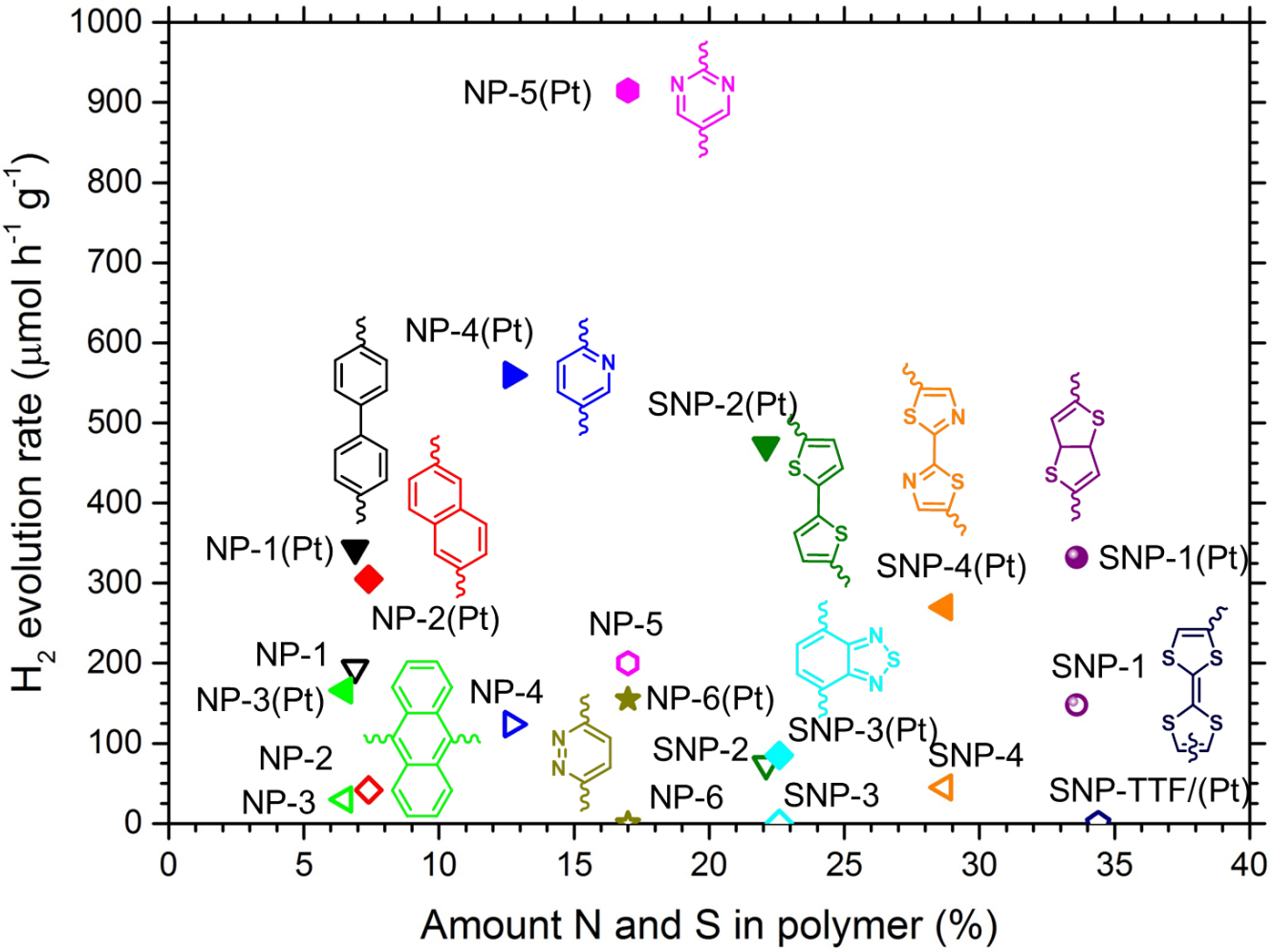

Figure S29. Hydrogen evolution rates of NPs, NNPs and SNPs in dependence of the amount of heteroatoms N and S in wt.% (N measured by combustion and S measured by ICP-OES). NP-1, NP-2, SNP-TTF, SNP-1, and SNP-2 were taken for comparison from the following reference. [17]

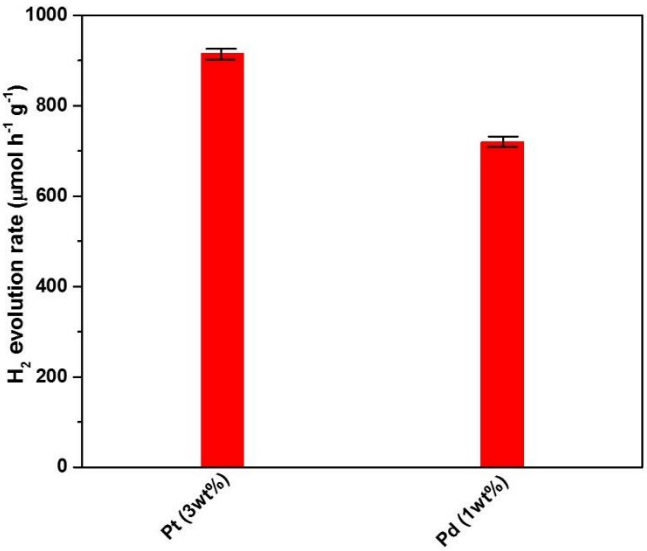

Figure S30. Influence of different co-catalysts (Pt, Pd) on hydrogen evolution rates of the best-performing NP-5 polymer.

Fluorescence

Time correlated single photon counting (TCSPC) and Photoluminescence measurements were carried out using a MicroTime 200 inverted confocal scanning microscope (PicoQuant, Germany) with a 100x air objective (UPLFLN, NA 0.9, Olympus, Japan). The spectra were recorded using an Andor SR 163 Spectrograph. For excitation, a picosecond pulsed laser head (LDH-405) with 405 nm center wavelength was used at 40 Mhz pulse rate with 1.6 µW excitation power. Life-time fitting was done using a double-exponential tailfit with SymphoTime 64 v 2.1 (PicoQuant, Germany). The samples were prepared by spreading the polymer powder as a thin film between two Menzelglass coverslips.

Table S12. Data of time-correlated fluorescence spectroscopy for NPs and SNPs.

sample	tau (ns)	A1 (kCnts)	Tau2 (ns)	A2 (kCnts)	Tau_avg (ns)
NP-3	4.28 ± 0.04	0.775 ± 0.015	1.015 ± 0.013	4.538 ± 0.028	1.492 ± 0.011
NP-4	3.912 ± 0.038	3.185 ± 0.066	1.071 ± 0.012	10.660 ± 0.062	1.725 ± 0.011
NP-5	1.147 ± .011	1.467 ± 0.011	4.131 ± 0.06	0.325 ± 0.011	1.689 ± 0.013
NP-6	1.076 ± 0.018	7.43 ± 0.04	3.749 ± 0.049	1.335 ± 0.046	1.483 ± 0.001
SNP-3	4.406 ± 0.056	0.570 ± 0.012	0.8850 ± 0.007	4.394 ± 0.043	1.289 ± 0.0078
SNP-4	0.94 ± 0.02	0.631 ± 0.012	3.95 ± 0.19	0.053 ± 0.005	1.17 ± 0.02

The life-times were estimated using a double-exponential function.

References

[1] D. Schwarz, Y. Noda, K. Schwarzova-Peckova, J. Tarabek, J. Rybacek, J. Janousek, F. Simon, M. V. Opanasenko, J. Cejka, A. Acharjya, J. Schmidt, S. Selve, V. Reiter-Schwerer, N. Severin, J. P. Rabe, P. Ecorchard, J. He, M. Polozij, P. Nachtigall, M. J. Bojdys, *Advanced Materials* **2017**, *29*, 1703399-1703399.

[2] A. Dondani, *Synthesis* **1987**, *2*, 185-186.

[3] J. Hassan, L. Lavenot, C. Gozzi, M. Lemaire, *Tetrahedron Letters* **1999**, *40*, 857-858.

[4] H. Usta,W. C. Sheets, M. Denti, G. Generali, R. Capelli, S. Lu, X. Yu, M. Muccini, A. Facchetti, *Chemistry of Materials* **2014**, *26*, 6542-6556.

[5] H. Bildirir, J.P. Paraknowitsch, and A. Thomas, *Chem. - Eur. J.* **2014**, *20*, 9543-9548.

[6] a) J. M. Soler, E. Artacho, J. D. Gale, A. Garcia, J. Junquera, P. Ordejon, D. Sanchez-Portal, *J. Phys. Condens. Matter* **2002**, *14*, 2745-2779; b) M. Brandbyge, J. L. Mozos, P. Ordejon, J. Taylor, K. Stokbro, *Phys. Rev. B* **2002**, *65*, 165401.

[7] J. P. Perdew, K. Burke, M. Ernzerhof, *Physical Review Letters* **1996**, *77*, 3865-3868.

[8] P. E. Blöchl, *Physical Review B* **1994**, *50*, 17953-17979.

[9] G. Kresse, J. Furthmüller, *Computational Materials Science* **1996**, *6*, 15-50.

[10] G. Kresse, D. Joubert, *Physical Review B* **1999**, *59*, 1758-1775.

[11] H. J. Monkhorst, J. D. Pack, *Physical Review B* **1976**, *13*, 5188-5192.

[12] S. Grimme, J. Antony, S. Ehrlich, H. Krieg, *The Journal of Chemical Physics* **2010**, *132*, 154104.

[13] G. Algara-Siller, N. Severin, S. Y. Chong, T. Björkman, R. G. Palgrave, A. Laybourn, M. Antonietti, Y. Z. Khimyak, A. V. Krasheninnikov, J. P. Rabe, U. Kaiser, A. I. Cooper, A. Thomas, M. J. Bojdys, *Angew. Chem. Int. Ed.* **2014**, *53*, 7450-7455.

[14] W.J. Gammon, O. Kraft, A. C. Reilly, B. C. Holloway, *Carbon* **2003,** *41*, 1917-1923.

[15] C. Li, C.-B. Cao, and H.-S. Zhu, *Materials Letters* **2004**, *58*, 1903-1906.

[16] C. Li, X. Yang, B. Yang, Y. Yan, Y. Qian, *Materials Chemistry and Physics* **2007**, *103*, 427-432.

[17] D. Schwarz, Y. S. Kochergin, A. Acharjya, A. Ichangi, M. V. Opanasenko, J. Cejka, U. Lappan, P. Arki, J. He, J. Schmidt, P. Nachtigall, A. Thomas, J. Tarabek, M. J. Bojdys, *Chemistry A European Journal* **2017**, *52*, 13023-13027.